Institut et hôpital neurologiques de Montréal
Montreal Neurological Institute and Hospital

Magneto-encephalography (MEG) to image the brain's role in the analgesic effects of Spinal Cord Stimulation (SCS)

Bart Witjes

9th of October 2018

Medical Sensing and Stimulation
Technical Medicine, University of Twente

Graduation committee

Prof. Dr. ir. M.J.A.M. van Putten
Drs. M.W.P.M. Lenders
Dr. ir. T. Heida
Dr. ir. C.C. de Vos
Drs. N.S. Cramer Bornemann

UNIVERSITY OF TWENTE.

Magneto-encephalography (MEG) to image the brain's role in the analgesic effects of Spinal Cord Stimulation (SCS)

Master Thesis

Bart Witjes

Technical Medicine

Medical Sensing and Stimulation

9th of October 2018

Graduation committee:

Prof. Dr. ir. M.J.A.M. van Putten
Chair, external member

Drs. M.W.P.M. Lenders
Medical supervisor

Dr. ir. T. Heida
Technical supervisor

Dr. ir. C.C. de Vos
Additional member

Drs. N.S. Cramer Bornemann
Process supervisor

Preface and acknowledgements

During my second M2 internship, I was first introduced to the neurosurgery department of the Medical Spectrum Twente. During that internship, I did EEG analysis of patients with a spinal cord stimulator and learned that I was really interested in this field of research. I was happy to be able to do my M3 internship at the same department, work with the same (and more) people and do further research in this field. The last year I have been working on this project with the goal to further exploring the cortical pain processing and the working mechanisms of spinal cord stimulation. Also, I was offered the opportunity to visit the MEG lab in Montreal and learned a lot about MEG data analysis. I really enjoyed working on this project, and I am really happy to be able to continue with the project after the completion of this thesis.

I would like to thank all my supervisors for their input and everyone that I have worked with for this project. A special thanks to Cecile de Vos, who has always made time to help me, showed me around in Montreal and introduced me to a lot of people, I really enjoyed working with her. I would also like to thank everyone in the MEG lab in Montreal for their help and teaching me how to use Brainstorm and their input for the project, specifically I would like to thank Elizabeth Bock and Martin Cousineau for answering all my questions. In addition, I want to thank everyone who participated in the study and everyone who helped with the measurements. I also like to thank the neurosurgeons and clinical staff of the MST neurosurgery department for giving me the opportunity to gain clinical experience. Last but not least, I would like to thank my girlfriend, Eline and my parents for their support.

Bart Witjes

Abstract

Background: Pain is a subjective experience and multiple factors play a role in the processing of pain. The network for the processing of pain, involving cortical and subcortical structures, has often been addressed in the neuroimaging of pain. Spinal cord stimulation (SCS) is used as a last-resort treatment for chronic neuropathic pain. Although there is plenty evidence that both, tonic and burst SCS, could be beneficial for neuropathic pain patients, the working mechanisms of SCS are still not fully understood. The goal of this study is to measure the neuronal activity in the pain processing brain areas and pathways involved in chronic neuropathic pain and assess how the different SCS settings affect the activity in these areas and pathways.

Methods: Resting-state magneto-encephalography (MEG) recordings were done in three groups of subjects: chronic pain patients (PC), subjects without pain (HC) and patients with SCS (PT). All subjects in the PT group evaluated one week of tonic, one week of burst and one week of placebo stimulation. The data analysis was two-fold: differences between HC and PC were analyzed, and the difference between different SCS settings were analyzed. For the HC and PC, the alpha power distribution was analyzed by computing a ratio of high theta power (7-9 Hz) and low alpha power (9-11 Hz). This was done at sensor level, and after source reconstruction. At source level, regions of interest (ROI) were defined and connectivity analysis was performed by computing the correlation and the coherence. For evaluation of the different SCS settings, the alpha power distribution was also analyzed at sensor and source level. The differences between SCS settings in power for the theta (4-7.5 Hz), alpha1 (8-10 Hz), alpha2 (10-12 Hz), beta1 (13-18 Hz), beta 2 (18.5-21 Hz) and beta3 (21.5-30 Hz) frequencies was also analyzed.

Results: Chronic pain patients showed significantly higher theta/alpha ratios predominantly at the right-sided sensors. Source reconstruction revealed significantly higher ratios in pain patients for the right insula, the mid-posterior and posterior cingulate cortex and the right S2. The coherence showed an increased connectivity between the right anterior insula and the right anterior S2. Comparing tonic to burst stimulation revealed a higher theta/alpha ratio during tonic stimulation for the temporal/occipital areas and the right insula. In addition, the somatosensory cortex and the parietal lobe showed increased alpha1 power for tonic stimulation. The power in the beta1 band for the somatosensory cortex and the parietal lobe was higher during burst stimulation.

Conclusion: An overall slowing of the alpha frequencies was found for the chronic pain patients, mainly in the right insula, the mid-posterior and posterior cingulate cortex and the right S2, suggesting the involvement of thalamocortical dysrhythmia (TCD). Burst stimulation seemed to reduce TCD to a larger extent than tonic stimulation. The differences at source level will have to be explored further in a larger number of subjects.

List of abbreviations

(A)CC	(Anterior) Cingulate cortex
BPI	Brief pain inventory
CPM	Conditioned pain modulation
CSF	Cerebrospinal fluid
DBS	Deep brain stimulation
DMN	Default mode network
DNP	Diabetic neuropathic pain
dSPM	Dynamical Statistical Parametric Mapping
ECD	Equivalent current dipole
ECG	Electrocardiogram
EEG	Electroencephalography
EOG	Electrooculogram
EQ5D-5L	EuroQ 5 dimensions questionnaire (5 levels)
FBSS	Failed back surgery syndrome
FDR	False discovery rate
FM	Fibromyalgia
FWER	Family-wise error rate
GABA	Gamma-amino butyric acid
HADS	Hospital anxiety and depression scale
HC	Healthy Controls
HNP	Herniated nucleus pulposus
IASP	International association for the study of pain
ISI	Interstimulus interval
MCP	Multiple comparisons problem
MCS	Motor cortex stimulation
MEG	Magneto-encephalography
MNE	Minimum norm estimates
MRI	Magnetic Resonance Imaging
MSR	Magnetically shielded room
NRS	Numeric rating scale
PC	Pain Controls
PCA	Principal component analysis
PCS	Pain catastrophizing scale
PSD	Power spectral density
PT	Patients (with SCS)
PVAQ	Pain vigilance and awareness questionnaire
ROI	Region of interest
S1	Primary somatosensory cortex
S2	Secondary somatosensory cortex
SCS	Spinal cord stimulation
SD	Standard deviation

SEP	Somatosensory evoked potential
SQUID	Superconducting quantum interference device
SSP	Signal-space projections
TCD	Thalamocortical dysrhythmia
VAS	Visual analogue scale
VEOG	Vertical electrooculogram

Contents

Chapter 1: Background

1.1 Pain

"Pain is an unpleasant sensory and emotional experience associated with actual or potential tissue damage, or described in terms of such damage." [1] This is the definition of pain, given by the international association for the study of pain (IASP) and acknowledges the multidimensional character of pain perception. Pain is processed through at least three different pathways: the ascending medial pathway, the ascending lateral pathway and the descending inhibitory pathway (fig 1). The medial pathway modulates the motivational, affective components of pain. It is activated by C-fibers, runs to the mediodorsal and ventral posterolateral nuclei of the thalamus and subsequently connects to the anterior cingulate and anterior insula respectively. The lateral pathway modulates the discriminatory components of pain. It is activated by C, Aδ and Aβ fibers, runs to the ventral posterolateral nuclei of the thalamus and connects to the somatosensory cortex and parietal area. The descending pathway suppresses ongoing pain. It connects the pregenual anterior cingulate cortex to the periaqueductal gray and then runs to the somatosensory periphery [2, 3]. So, cortical and subcortical structures are involved in the perception and processing of pain. This network has been referred to as the 'pain matrix' and has often been addressed in the neuroimaging of pain [4].

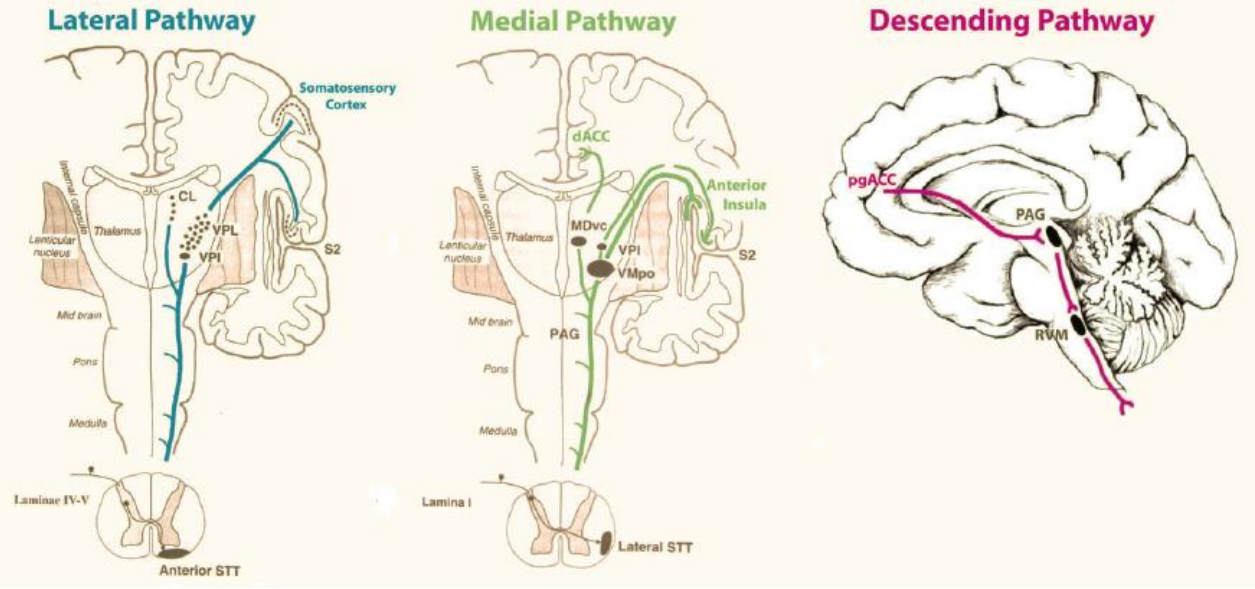

Figure 1: Schematic overview of three pain processing pathways: the lateral, medial and descending pathways. The lateral pathway processes the discriminatory components of pain, the medial pathway processes the motivational, affective components of pain and the descending pathway suppresses ongoing pain. Figure from de Ridder et al. [5].

Neuropathic pain is a type of pain caused by a lesion or dysfunction of the nervous system [1]. A common cause of neuropathic pain is a herniated nucleus pulposus (HNP), whereby the intervertebral disc is degenerated, causing the soft, gelatinous portion of the disc (the nucleus pulposus) to prolapse. When the HNP compresses a nerve, it causes neuropathic pain. Patients with neuropathic pain typically suffer from continuously burning pain that occurs spontaneously. This can be accompanied by other sensations such as tingling or itching, also called dysesthesia. Other symptoms that can occur are an increased response to a normally painful stimulus (hyperalgesia) or

the sensation of pain due to a stimulus which is normally not painful (allodynia) [6]. Common treatment options of neuropathic pain are pharmacological options or, if possible, surgical intervention. However, these options do not always result in the desired pain relief.

1.2 Spinal Cord Stimulation

Spinal cord stimulation (SCS) is used as a treatment for chronic neuropathic pain, for example in the case of failed back surgery syndrome (FBSS) and diabetic neuropathic pain (DNP). Patients with FBSS still suffer from persistent neuropathic pain although they already had spinal surgery. This mostly involves lumbosacral spinal surgery for the treatment of spinal stenosis, with or without HNP [7]. DNP is caused by poor perfusion due to diabetes mellitus and is mostly presented as persistent pain in the feet and lower legs.

For SCS therapy, an electrode lead is placed in the epidural space over the dorsal columns of the spinal cord. A current is applied via this electrode, which results in pain relief in the dermatome innervated by the stimulated nerves. The precise working mechanism behind SCS is not completely understood, but there are several theories. The assumed main working mechanism is the gate control theory, which was proposed in 1965 by Melzack and Wall [8]. The gate control theory suggests that stimulation of the dorsal horn results in activation of the large Aβ-fibers, which blocks the pain signal that is transmitted by smaller Aδ and C fibers. The activation of the Aβ-fibers produces a tingling sensation (paresthesia) in the innervated dermatome, but ideally patients do not perceive the pain in that dermatome anymore [5, 9, 10]. SCS might work through antidromic activation of the ascending pathways, but could also work through orthodromic activation of the descending pathway. In addition, some animal studies suggest that the stimulation of A-fibers results in the release of gamma-amino butyric acid (GABA), which results in pain suppression at the spinal level by local interneurons [10].

Currently, there are two general stimulation settings used in SCS: tonic stimulation and burst stimulation. Conventional tonic stimulation is generally programmed with an amplitude between 2 and 15 mA, a pulse width between 0.1 and 0.5 ms and a frequency between 30 and 80 Hz [11, 12]. Nowadays, also high frequency tonic stimulation is used, with frequencies up to 10 kHz [13]. Burst stimulation generally has a lower amplitude and a larger pulse width compared with conventional tonic stimulation. For burst stimulation the pulses are delivered in packages (bursts) of five pulses, alternated with a resting period. The bursts are delivered with a frequency of 40 Hz, with the five pulses at 500 Hz [9]. Although conventional tonic stimulation is accompanied by paresthesia, both high frequency stimulation and burst stimulation can achieve pain relief without the occurrence of paresthesia.

1.3 Magneto-encephalography

To visualize the effects of pain and its treatment by SCS, we can analyze the brain activity. Magneto-encephalography (MEG) is a method to study brain activity by capturing the magnetic fields generated by the electric currents of the brain. The method is similar to electroencephalography (EEG), which measures the dendritic currents of groups of pyramidal neurons that fire

synchronously and in parallel, directly [14]. MEG measures the activity of the same type of cells, but instead of measuring a potential difference between two electrodes, it measures the magnetic field that is evoked by large assemblies of neurons, which fire synchronously and in the same direction [14].

As the magnetic fields, generated by neuronal currents, are very small (of the order of several tens of femto Teslas), the MEG sensors have to be very sensitive. To acquire this sensitivity, the MEG scanner uses superconducting quantum interference devices (SQUIDs) to capture the cortical activity. Liquid helium is used to create the extremely cold environment that is necessary for super conduction. As the sensitivity of the sensors is very high, the MEG signal is easily contaminated with noise. To minimize the influence of noise, MEG measurements are conducted in a magnetically shielded room (MSR) and subjects should not have any form of magnetic metals in or on their body (for example, dental work).

Source localization is the principle whereby the source of the MEG signal is estimated. Source localization involves two main models: a forward model and an inverse model. The forward model consists of two parts: a source model, which explains how the neural electrical currents produce a magnetic field, and a volume conductor model, which explains how this magnetic field is transmitted through the tissues to the MEG sensors. A commonly used approach for the source model is the equivalent current dipole (ECD) approach, whereby multiple current dipoles represent post-synaptic electrophysiological activity of groups of neurons. A volume conductor model is then used to describe the electrical properties of the tissue and explain how the currents flow towards the MEG sensors. An advantage of MEG is that the magnetic fields are not affected by the cerebrospinal fluid (CSF) and the skull, whereas these factors do distort the EEG signal. Therefore, simplified volume conductor models can be used for MEG [14, 15].

The inverse model explains where the MEG signals are coming from. In the case of an ECD source model, we want to know which current dipoles produce which part of the MEG signal. However, we have a large number of current dipoles and a much smaller number of MEG sensors: this is called the inverse problem. Although there is no true solution to the inverse problem, there are multiple methods that approach a solution. An example of such an approach is the minimum norm estimate: this model minimizes the error between the source model and the recorded MEG signals [14, 15].

Compared to EEG, MEG has the advantage of a better spatial resolution of source localization: MEG has a spatial resolution of 2-3 mm whereas EEG has a spatial resolution of 7-10 mm. Together with the very good temporal resolution of MEG, this enables the possibility to study the activity of specific brain areas more closely. However, due to its need for liquid helium, MEG is a much more expensive technique than EEG and it is not often used for clinical applications [14].

Chapter 2: Rationale

2.1 Spinal cord stimulation

During my previous internship at the neurosurgery department, we used EEG data to study the effect of SCS on the activity of the brain [16]. The goal of that internship was to examine whether the brain activity of chronic pain patients treated with SCS showed the same feature as previously described by Schulman et al. [17]: a slowing of the alpha frequencies towards the theta frequencies in chronic neuropathic pain patients. To quantify slowing of alpha frequencies, they defined a theta/alpha ratio as the power in the high theta frequency band (7-9 Hz) divided by the power in the low alpha band (9-11 Hz). They found an increased theta/alpha ratio for neuropathic pain subjects and failed SCS subjects, which was similar to the ratio of subjects with thalamocortical dysrhythmia (TCD) disorders. For successful SCS subjects however, the theta/alpha ratio was comparable with control subjects without pain. This caused the authors to believe the processing of pain works differently for subjects for whom SCS is not successful, compared to the subjects for whom SCS is successful. The main finding of my previous internship was in line with Schulman et al: patients, in whom SCS did not result in pain relief (subjects in pain), showed a relatively higher power in the theta frequency band and lower power in the alpha frequency band, than the control subjects without pain. However, these results were not statistically significant due to the limited number of subjects and the variation between subjects was very large. Schulman et al. reported on a limited number of subjects as well.

Another point of interest during my previous internship was the working mechanisms of two different stimulation settings; conventional tonic and burst stimulation. This was first studied by de Ridder et al. [5, 9]: during the trial stimulation phase of SCS, they tested one-week evaluation periods of tonic, burst and placebo (stimulator turned off) stimulation and recorded an EEG after each week of evaluation. They compared the EEGs of five subjects, wherefore the results showed more alpha activity in the dorsal anterior cingulate (which is a component of the medial pain pathway) during burst stimulation, compared to the other stimulation settings. Therefore, they suggested that burst stimulation modulates the lateral pathway and the inhibitory pathway, but also the medial pathway, whereas tonic stimulation only modulates the lateral pathway and the inhibitory pathway. During my previous internship I could not reproduce these results.

Although there is plenty evidence that both, tonic and burst stimulation, could be beneficial for patients with neuropathic pain, the working mechanisms of SCS are still not fully understood [12, 18]. It remains unclear which patients could benefit from SCS (either tonic or burst stimulation) and which patients could not. As (depending on the etiology) up to 35% of the chronic pain patients do not benefit from SCS, it is important to understand its working mechanisms, to be able to predict for whom it would be beneficial and to further improve and personalize the treatment of chronic neuropathic pain.

2.2 Chronic pain

Pain is a subjective experience and multiple factors play a role in the processing of pain. Already several different pain processing pathways and specific brain areas have been mentioned for their involvement in the processing of pain. In addition, it has been suggested that somatosensory processing is altered for chronic pain patients [19-21]. There are multiple studies whereby electrophysiological measures such as EEG have been used to try and objectify these alterations.

One of the reported alterations in EEG and MEG for chronic pain is slowing of the dominant rhythm [22]. For example, Schulman et al. described a shift of alpha peak frequency towards lower frequencies (theta) for chronic pain patients [17]. They compared resting state MEG recordings of subjects with deafferentation pain syndromes, subjects who had received SCS which resulted in pain relief and subjects who had received SCS which did not result in pain relief. They analyzed the shift of the alpha peak by computing a ratio of power in the high theta band (7-9 Hz) and power in the low alpha band (9-11 Hz) and found that deafferentation pain patients and patients for whom SCS was not successful, showed a larger shift from alpha frequencies towards theta frequencies. The shifting of the dominant (alpha) rhythm towards the theta frequencies is often described to thalamocortical dysrhythmia (TCD). TCD is described as a decreased inhibition of the thalamus, which causes an increased theta activity that reduces lateral inhibition, causes an increased gamma activity and therefore causes abnormal pain processing [17, 20, 22-24].

Possibly, the slowing of the dominant rhythm could be used to generate an electrophysiological marker of chronic pain. However, general slowing of the dominant rhythm has also been described in other neurological and psychiatric disorders (for example Alzheimer's disease) and might not be specific enough [22, 25]. When more is known about the processing of chronic pain at the cortical level, it might also give better insights into the working mechanisms of SCS. At this moment, there is no clear, objective marker which describes the altered cortical activity of chronic pain patients yet. Such a marker would be useful to objectify, monitor or predict the effect of the treatment of pain, and to monitor or predict whether SCS in general or which stimulation settings in particular would be beneficial for an individual patient.

2.3 Aim of the study

The overarching goal of this project is to measure the neuronal activity in the brain areas and pathways that are involved in the processing of chronic neuropathic pain and assess how the different SCS settings affect the activity in these areas and pathways. As a first step to accomplish this goal, I proposed several objectives for this thesis:

- Study with MEG whether there is a shift in power from alpha frequencies towards theta frequencies for chronic pain patients compared to control subjects without pain
- Study which brain areas show this shifting of alpha frequencies towards theta frequencies, using a MEG source model.
- Study how these brain areas relate to each other, using connectivity measures in the time domain and the frequency domain.

- Study with MEG whether there is a difference in shifting of the alpha frequencies as a result of different SCS settings: tonic stimulation and burst stimulation.
- Study which brain areas show this shifting of alpha frequencies as a result of the different SCS settings, using a MEG source model.
- Study in which brain areas activity in specific frequency bands is altered as a result of the two different SCS settings, using a MEG source model.

The project will be continued after the completion of this thesis, and subsequent objectives will be proposed to accomplish the primary goal. Eventually, we hope to develop a MEG based pain signature, which is able detect chronic neuropathic pain and ideally predict whether SCS would be beneficial for a patient or not.

Chapter 3: Methods

To achieve the goals described in 2.3, the study was divided into two parts. First, the differences in cortical activity between chronic pain patients and subjects without pain were analyzed. Second, the cortical activity of patients with a spinal cord stimulator was analyzed. After that, the results for the three different groups were compared. The data acquisition for all three groups was done in the same way, but the measurement protocol was different for the SCS patients as they evaluated three different stimulation settings.

3.1 Study groups

In total, three groups of subjects were recruited for this study; a group of chronic pain patients, a group of subjects without pain and a group of SCS patients. Because the overall goal is to study the effects of spinal cord stimulation, the groups of chronic pain patients and subjects without pain will be referred to as control groups. The three study groups and their inclusion criteria were as follows:

- Subjects without chronic pain (Healthy Controls, HC): no pain and no other neurological disease, but moderate, non-painful other medical conditions were not an exclusion criterion.
- Chronic pain patients (Pain Controls, PC): chronic neuropathic pain in the lower body part and preferably on a waiting list for a SCS implant. Subjects who also suffered from (severe) pain in another body part or another form of serious decline of general health, were excluded.
- SCS patients (Patients, PT): a SCS system which is capable of burst stimulation and already experienced more than three months of stimulation. Subjects who also suffered from (severe) pain in another body part or another form of serious decline of general health, were excluded.

3.2 Data acquisition

MEG was used to record the cortical activity of the three groups. The recordings were done at two locations; the Montreal Neurological Institute (MNI, Montreal, Canada) and at the Donders Institute for Brain, Cognition and Behavior (Nijmegen, the Netherlands). The MEG system, the acquisition software and the measurement setup were the same for both locations. The subjects were measured in seated position with a 275-channel whole-head MEG system (CTF, Coquitlam, BC, Canada) inside a magnetically shielded room (MSR). The sensors and their distribution across the helmet are shown in figure 2. Before entering the MSR, the subjects were instructed to remove any metal materials that could distort the measurements. Recordings were made with a sample rate of 2400 Hz and the 3rd order gradient compensation was applied for noise reduction. In order to detect eye blinks and cardiac artifacts, horizontal and vertical electrooculogram (EOG) and electrocardiogram (ECG) were recorded simultaneously during the MEG recording. To detect the subject's head position in the MEG helmet before each recording, coils were attached close to three anatomical landmarks: the nasion and the left and right pre-auricular points. A 3-D digitizer system (Polhemus Isotrack) was used to digitize the subject's head shape, the location of the coils and the true location of the anatomical landmarks. Before a subject entered the MSR, a two-minute empty-room

recording was made to capture the environmental noise. The noise recording was used for the noise cancellation in the process of source reconstruction (section 3.3.3).

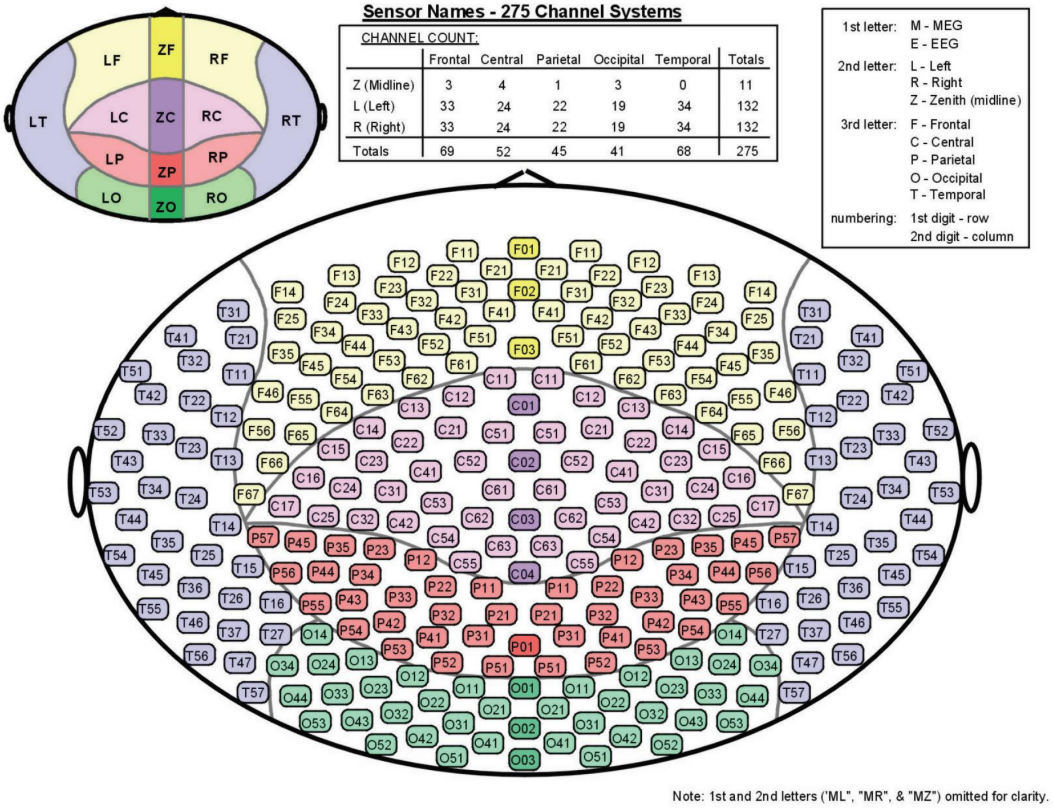

Figure 2: The distribution of sensors in the helmet of the CTF 275-channel whole-head MEG system.

In the MEG, three conditions were tested; the resting state cortical activity, the cortical response to somatosensory evoked stimulation (somatosensory evoked potential, SEP) and the response to conditioned pain modulation (CPM). Because recording and cleaning the data (section 3.3.1) was very time-consuming, only the data of the first resting state recordings was analyzed for this thesis. For a better overview of the complete setup, the other conditions are explained briefly.

3.2.1 Measurement protocol HC and PC

The HC subjects and the PC subjects underwent one MEG session, which consisted of seven short recordings; one resting state recording in the beginning, two SEP recordings, three recordings for the CPM test and one resting state recording at the end. Before each session, the subjects were asked to fill in several questionnaires: the brief pain inventory (BPI), the pain catastrophizing scale (PCS), the EuroQol 5 dimensions 5 levels (EQ5D-5L), the hospital anxiety and depression scale (HADS) and the pain vigilance and awareness questionnaire (PVAQ). Each subject was offered to fill in the questionnaire in their own language (either Dutch, English or French). For this thesis, only the

results of the BPI were used to obtain the pain intensity for each subject. The pain intensity was expressed with the numeric rating scale (NRS), whereby 0 is no pain and 10 is the worst pain imaginable.

Resting state recordings: the participants were instructed to sit still, keep their eyes open, relax and to focus on a fixation cross. This recording lasted five minutes. The instructions and the fixation cross were presented to the subjects on a screen in the MSR. The presentation was made in Matlab, using the Psychophysics Toolbox extensions [26, 27].

SEP recordings: approximately 200 stimuli were applied to the median nerve (the first SEP recording) and the tibial nerve (the second SEP recording) with a randomly varying interstimulus interval (ISI) between 0.7 and 1.5 seconds. The stimuli were applied with a constant current electrical stimulator (Digitimer Ltd), which was programmed to deliver the stimuli with varying ISI using Matlab (The MathWorks, Massachusetts, USA). We used a pulse width of 200 microseconds and an amplitude level which was just high enough for eliciting a twitch. Subjects were instructed to silently count the number of stimuli, to ensure that the attention of the subjects was on the stimuli. After each SEP recording, we asked the subjects for the number of stimuli that they had counted, and they received feedback on their accuracy.

CPM recordings: the test consisted of three recordings, whereby each time 22 unpleasant stimuli were applied to the tibial nerve with a randomly varying ISI between 6 and 10 seconds. The stimuli consisted of a burst of 5 pulses each with a pulse width of 200 microseconds and with 5 milliseconds between each pulse. The amplitude of the stimuli was individually adjusted to the point where the subject indicated a pain score around 5 out of 10 (where 0 is no pain and 10 is the worst pain imaginable). During the first recording, only the stimuli were applied. During the second recording, the stimuli were applied in combination with an icepack on the left hand and forearm. After that, a third recording was done with the stimuli but without the icepack, to measure the extinction of the cold pressor test [28, 29].

3.2.2 Measurement protocol PT

To assess the effect of different stimulation settings on the cortical activity, the SCS patients underwent four MEG sessions. During the first session, a baseline recording was made with their own stimulation settings, after which the stimulation settings were changed to either tonic, burst or placebo stimulation. The type of stimulation was randomly chosen and neither the patient nor the researchers knew the type of stimulation. After this, the direct effects of the change of stimulation were recorded. One week later, the long-term effects of the change of stimulation were recorded with another MEG session (whereby the procedure of the first MEG session was repeated). Before each session, the subjects were asked to fill in the questionnaires (BPI, PCS, EQ5D-5L, HADS and PVAQ). From the BPI questionnaire, the NRS scores were used to indicate the pain intensity of the subjects.

A MEG session for SCS patients started with a resting state recording of 5 minutes, followed by two recordings of SEPs (again, one with median nerve stimulation and one with tibial nerve stimulation)

and the CPM test. After this, the stimulation settings were changed to the next settings and another resting state recording of 5 minutes was done, followed by the two SEP recordings. During the fourth MEG session, the stimulation settings were not changed, therefore the session ended with a resting state recording only.

3.3 Data Analysis

The data analysis was performed with Brainstorm[30], which is documented freely and available for download online under the GNU general public license (http://neuroimage.usc.edu/brainstorm). All the steps that are explained in this chapter, are built-in options in Brainstorm. To learn about the possible steps and their technical background, I used the tutorials which are documented on their website. As mentioned before, these analyses were performed on the first resting state recording for every subject only.

Before any data analysis could be performed, the data had to be cleaned. Subsequently, the data analysis was performed in two parts. The first part of the data analysis consisted of analyzing the differences in cortical activity between pain and no pain, wherefore I looked at the following measures: the alpha power distribution; at sensor level, at source level and at specific brain regions of interest (which are known to be involved in pain processing). Also, I analyzed the connectivity between those specific areas by computing the correlation and the coherence between the specific areas. The differences were quantified using the statistical tests for MEG, available in Brainstorm. The second part consisted of analyzing the differences in cortical activity within the SCS group as a result of the different stimulation settings. For this part, also the alpha power distribution (at sensor level and at source level) was analyzed. To be able to compare the results with de Ridder et al. [5, 9], the differences in specific frequency bands for the different stimulation settings were analyzed.

3.3.1 Data cleaning

Because of the large number of artifacts, each resting state recording was first visually inspected and cleaned manually. The inspection was done in the time domain, and in the frequency domain by computing the power spectrum density (PSD) using Welch's method with a 4 second window and 50% overlap. Individual or small groups of sensors that showed unexpectedly deviant behavior from their surrounding sensors, were marked as bad and excluded for further analysis.

Notch filters

Powerline artifacts were removed by applying a notch filter at the powerline's frequency and its higher harmonics (50, 100 and 150 Hz at the Donders and 60, 120 and 180 Hz at the MNI). For the PT group, the SCS could also cause artifacts in the MEG signal, as the SCS stimulates with an electrical current (and therefore also creates a magnetic field). Although varying for individual patients, the frequency of the stimulation was always of a set frequency and therefore clearly visible in the PSD. This frequency, and its higher harmonics, could also be removed with a notch filter. In rare cases, the notch filter did not work sufficiently, in which case a narrow band-stop (for example 39-40 Hz) filter was used.

Frequency filters

If deemed necessary, a bandpass filter was applied to remove low (< 1 Hz) and high (> 200 Hz) frequency noise. Low frequency noise could occur as a result of any form of metal in the subject's body (for example, dental work); breathing causes these metals to generate a low frequency oscillation in the MEG signal. High frequency noise could occur as a result of muscle activity due to movement of the subjects. Muscle activity can be seen in the MEG signal at frequencies between 20 and 300 Hz [31], but the muscle activity lower than 200 Hz was not removed by using a lowpass filter, to prevent removing actual brain activity. The muscle activity below 200 Hz was removed differently, as will be explained in the next paragraph.

Principle component analysis (PCA)

The heart beat and eye movements cause artifacts in the MEG signal. The cardiac artifacts and the eye blinks, but also the muscle activity, were removed by using principal component analysis (PCA) [32, 33]. For the removal of the cardiac artifacts, the R-peaks in the ECG were detected and selected as an event. For the removal of the eye blinks, the peaks in the vertical EOG were selected as an eye blink event. If the recording was contaminated with multiple saccades, the horizontal EOG was used to mark the saccades as events. The events for muscle activity were selected either by automatic detection of data segments with an increased amplitude of frequencies between 40 and 240 Hz, or manually. After the detection of events, PCA was used to compute signal-space projections (SSPs) from these events. The resulting SSPs were topographies which represented the spatial distribution of the signal at the given events. For the SSPs which were similar to the artifact topography (for example, eye blinks occur at the most frontal sensors only), a linear projector was computed to remove this contribution from the signal. Artifacts whereby no sufficiently resembling SSP could be computed, were marked as 'bad' and these segments were excluded from further analysis.

3.3.2 Alpha power distribution: sensor level

The first measure that was calculated, was the measure described by Schulman et al. [17]; a shift of alpha frequency power, towards the lower theta frequencies due to neuropathic pain. A PSD was calculated for every sensor, using Welch's method, with a 4 second window and 50% overlap. Subsequently, the power of the frequencies in the high theta band (7-9 Hz) and the power of the frequencies in the low alpha band (9-11 Hz) were extracted (for every sensor). The theta/alpha ratio was then calculated by dividing the power in the theta band by the power in the alpha band. To observe the group differences, an average ratio across all subjects in a group was calculated for each of the 275 sensors and visualized with a colormap in a schematic head: a theta/alpha ratio topography. As the final goal is to be able to distinguish between pain and no pain at an individual level, also the individual theta/alpha ratio topographies were computed.

In the paper of Schulman et al. the average theta/alpha ratio across the whole head was computed. To be able to compare our results with the literature, this was also done for our subjects. The average ratio across all sensors was calculated for each subject and the differences between the two groups were compared. To validate if the ratio could classify the subjects in the two groups, a cut-off value was determined by plotting a receiver operating characteristic (ROC) curve (using SPSS version 24.0). The sensitivity and the specificity were both maximized, using Youden's index [34].

3.3.3 Alpha power distribution: source level

For a better determination of the brain areas contributing to the MEG signal, the data was analyzed at source level. First, the MEG signal was linked to an MRI. If an individual MRI was available for the subject, the subject's own anatomy was used. If there was no MRI available, the default ICBM152 MRI was used, and warped to the subject's head, using the digitized head shape which was made before each recording. The MRI was used to perform cortical reconstruction and volumetric segmentation with the FreeSurfer image analysis suite, which is documented and freely available for download online (http://surfer.nmr.mgh.harvard.edu/). The result of the FreeSurfer software was the cortical surface extracted from the MRI [35]. This cortical surface was then imported into Brainstorm and downsampled to 15000 vertices. These vertices represent the number of dipoles to estimate during the source estimation process. To ensure a correct position of the head model in relation to the MEG helmet, 6 fiducial points (the nasion, the left- and right pre-auricular points, the anterior- and posterior commissure and an interhemispheric point) were marked in the MRI. Those points were then used to match with the anatomical points which were marked in the digitized head shape. The product of these steps was a cortical surface consisting of 15000 vertices, with a known position in relation to the MEG helmet.

The brain activity in the cortical surface was modeled in a current dipole model: one current dipole represents the post-synaptic electrophysiological activity of a group of neurons. To reduce computation time, the model was simplified, and the positions and orientations of the current dipoles were constrained. The positions of the current dipoles were set at the locations of the 15000 vertices, and the orientations were set perpendicularly with respect to the cortical surface (assuming that the measured fields are produced by apical dendrites, which are oriented normal to the surface) [15, 36]. The next step was to create a forward model; a model which explained how the MEG sensors capture the activity of the groups of neurons (the current dipoles). As MEG is less sensitive to the different head tissues (white and grey matter, cerebrospinal fluid, skull bone and skin) compared to EEG, the forward model was also simplified. For each MEG sensor, a sphere was estimated which represents the shape of the inner skull. In the end, the model consisted of overlapping spheres for each of the 275 MEG sensors [37].

Subsequently, the forward model was used to estimate the activity of the current dipoles, or in other words, to estimate the sources of the MEG signal. This is an inverse problem; we have the results (the MEG signal), but we have to compute the cause (the activity of the dipoles). The minimum norm imaging method of Brainstorm was used as a solution to this problem. This method minimizes the sum of the squared residuals of the source estimate, while trading off between reconstruction of the data and suppression of the noise [38]. In order to do this, a noise covariance matrix was estimated from the noise recordings, which were recorded before each MEG session (the same notch- and frequency filters that were applied to the actual data, were applied to the noise recordings). The advantage of the minimum norm estimates (MNE) is that it is a relatively simple method to compute the sources, but it also tends to place source activity at the surface of the cortex. To reduce this effect, the results were normalized by applying dynamical statistical parametric mapping (dSPM) [39]. This method normalizes the results for the MNE, based on the noise covariance matrix. This

resulted in source maps with values which were similar to z-scores and represented the measure of activity for each source.

The source maps were used to extract the alpha power distribution for every source. To reduce computation time, the PSD was only computed for the high theta band (7-9 Hz) and the low alpha band (9-11 Hz). Furthermore, the alpha power distribution was computed the same way as for the sensor level (described in 3.3.2).

3.3.4 Specific brain areas

The alpha power distribution was also computed for specific brain regions of interest (ROIs), which are known to be a part of the pain processing network [2, 3]. This was done to study whether there is a relation between the ROIs and the alpha power distribution. The areas that were studied more closely were: the prefrontal cortex, the insular cortex (anterior and posterior), the primary somatosensory cortex (S1), the secondary somatosensory cortex (S2, anterior and posterior) and the cingulate cortex (CC, anterior, mid-anterior, mid-posterior and posterior).

The source maps, that were obtained after the source reconstruction (see previous section), were used for analyzing the activity of the ROIs. The ROIs were defined by an assembly of sources on the cortical surface, which were situated in these brain areas. The Destrieux atlas, which is a parcellation scheme in FreeSurfer, was used to create these ROIs on the cortical surface [40, 41]. When the ROI from the Destrieux atlas did not completely cover the brain area, or cover more than the intended area, the ROI was modified in Brainstorm. The sources that represented the ROI are shown in appendix A. For each ROI, the average PSD across all sources in that ROI was calculated (again, for the high theta band (7-9 Hz) and the low alpha band (9-11 Hz) only). Subsequently the theta/alpha ratio was computed (section 3.3.2).

The same ROIs were used to analyze their connectivity. This was done by using two different measures; the correlation between the ROIs and the coherence between the ROIs. The correlation was computed for every subject by first computing the average time series for each ROI and then computing Pearson's correlation coefficient between these 5-minute time series at zero lag. This resulted in a correlation coefficient, whereby a coefficient of -1 indicates a perfect negative linear relation between the two ROI and a coefficient of 1 indicates a perfect positive linear relation between the two ROI [42]. As the direction of the correlation was assumed to be of less importance and to improve the interpretability, the absolute values of the correlations were taken. The absolute correlation values per ROI were then averaged for each group. For the coherence, the PSD for each ROI was computed with a frequency resolution of 0.6 Hz. Subsequently, the PSDs of two ROIs (x and y) were compared by computing the magnitude squared coherence (COH_{xy}). This was done by dividing the cross spectral density between the two ROIs (S_{xy}) by the PSDs of the two ROIs (S_{xx} and S_{yy}) [42]:

$$COH_{xy}(f) = \left|K_{xy}(f)\right|^2 = \frac{\left|S_{xy}(f)\right|^2}{S_{xx}(f)\, S_{yy}(f)}$$

The differences in coherence between the two groups were analyzed for the high theta band (7-9 Hz) and the low alpha band (9-11 Hz). As I selected a total of 16 ROIs (the mentioned brain areas for the left- and right hemisphere, the sources for the cingulate cortex were assumed to be in the middle), this resulted in averaged 16x16 connectivity matrices (for the correlation and for the coherence) for each group. To evaluate the differences, the connectivity matrices for the PC group were subtracted from the connectivity matrices for the HC group.

3.3.5 Statistical analysis

For performing statistical tests on the MEG data, I had to take into account the multiple comparisons problem (MCP). In the time domain for example, the data of two groups was compared for all 275 sensors at a lot of time points. This increases the chance of finding false positives; it increases the family-wise error rate (FWER). In Brainstorm, the nonparametric permutation test was used, because this method is more suitable to control for the FWER [43, 44].

For the nonparametric permutation test, first the trials of the HC group and the PC group were collected in a single set (resulting in 42 trials in total). Second, 21 trials were randomly selected from this set and put in subset 1, the rest was put in subset 2 (causing the HC and the PC to be mixed). Third, a two-tailed student's t-test was performed between these subsets. Subsequently, the second and the third step were repeated 1000 times (1000 permutations) and a histogram was constructed of the test statistics. To reduce computation time, the Monte Carlo approach with only 1000 permutations was used. Therefore, this histogram only approximates the permutation distribution. The p-value was then determined by comparing the histogram and the observed test statistic (the t-test between the actual HC and PC). The p-value was the proportion of permutations that resulted in a larger test statistic than the observed statistic [43, 44].

To control for the FWER, the false discovery rate (FDR) correction was used, which corrected for the number of signals (the number of sensors or sources). The FDR corrected p-value represents the percentage of false positives of the significant values (without correction, the p-value represents false positive of all values) [45]. The corrected p-values were considered significant when they were smaller than 0.01.

Statistical analysis was performed only for the first part (comparing the HC and the PC). The permutation test was used to analyze the difference between the two groups for the following measures: the theta/alpha ratio topographies (section 3.3.2), the theta/alpha ratio for the sources and the theta/alpha ratio for the ROIs. For the second part (comparing the different stimulation settings of SCS), statistical analysis was not performed due to the low number of subjects.

3.3.6 Spinal cord stimulation

The third part of the analysis consisted of evaluating the effects of SCS and its different stimulation settings. Therefore, for every subject in the PT group, the resting state recordings of the three 1-week evaluation periods were analyzed. This was done by looking at some of the same measures as for the first part (pain vs no pain) and by looking at specific frequency bands.

The alpha power distribution for the sensors (section 3.3.2) and the alpha power distribution for the sources (section 3.3.3) were computed and averaged for each stimulation setting (tonic, burst and placebo). To observe the differences between the stimulation settings, these three averages were subtracted from each other. This resulted in three figures for each measure: the differences between tonic and burst, between tonic and placebo, and between burst and placebo. Due to the low number of subjects, statistical analysis was not performed for this part of the analysis.

To compare our results with the results that have been published by De Ridder et al. [5, 9], for every PT subject the differences in cortical activity, as a result of the different stimulation settings, were analyzed at the following frequency bands: theta (4-7.5 Hz), alpha1 (8-10 Hz), alpha2 (10-12 Hz), beta1 (13-18 Hz), beta 2 (18.5-21 Hz) and beta3 (21.5-30 Hz). For every source, the mean frequency for each band was calculated and normalized by dividing the mean frequency of a band by the total power within all of these frequency bands. Subsequently, the results were averaged for each of the three stimulation settings and those means were subtracted from each other for a comparison (resulting in again three comparisons: tonic-burst, tonic-placebo and burst-placebo). Statistical analysis was not performed for this part either, due to the low number of subjects.

Chapter 4: Results

4.1 Pain vs. no pain

For the HC group, 21 subjects (8 females) were included. For the PC group, also 21 subjects (10 females) were included. The mean age and standard deviation (SD) were 47 ± 11 years old for the HC group and 48 ± 10 years old for the PC group. The NRS pain score was 0 ± 0 for the HC group and 5.5 ± 2.4 for the PC group. From the PC group, 38% suffered from pain in both (left and right) legs, 33% suffered from pain in their left leg (and not their right), 14% suffered from pain in their right leg and 14% suffered from pain in their back only.

4.1.1 Alpha power distribution: sensor level

The results for the average theta/alpha ratio at each sensor for both groups are shown in figure 3. The ratio topography for the HC (left) showed ratios primarily below 1, which means that there is more power in the 9-11 Hz frequency band than in the 7-9 Hz frequency band. The ratio topography for the PC (right) showed ratios primarily above 1, meaning more power in the 7-9 Hz band than in the 9-11 Hz frequency band.

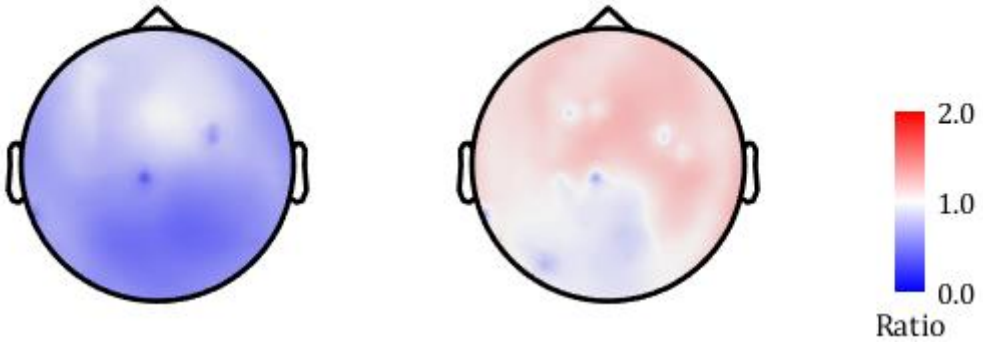

Figure 3: The theta/alpha ratio for each of the 275 sensors. The ratio topographies are shown for (left) the healthy controls and (right) the pain controls. The values represented in the figure are the theta/alpha ratios, a higher ratio means more power in the 7-9 Hz frequency band and a lower ratio means more power in the 9-11 Hz frequency band.

The statistical differences between the two groups are shown in figure 4. In this figure, only the sensors that were significantly different ($p < 0.01$) between the two groups were highlighted. A positive t-value corresponds to a higher ratio for the HC, a negative t-value corresponds to a higher ratio for the PC. The PC group showed a statistically significant higher ratio (more power in the high theta band) for the central and parietal (left and right), and the right temporal and occipital sensors.

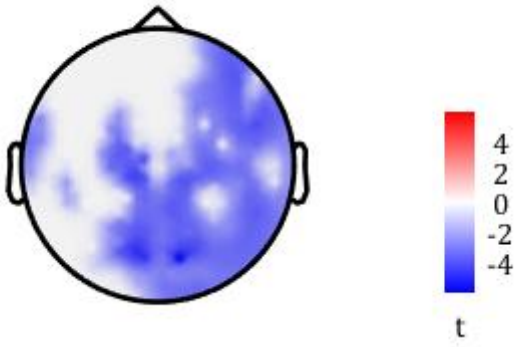

Figure 4: The results for a permutation t-test between average (sensor level) theta/alpha ratios for the healthy controls (HC) and the average (sensor level) theta/alpha ratios for the pain controls (PC). The values represented in the figure are t-values based on a significance level of $p < 0.01$, a high t-value means a higher ratio for the HC and a low t-value means a higher ratio for the PC. The results were false discovery rate (FDR) corrected for the number of sensors.

The individual ratio topographies (shown in appendix B.1) revealed that the topography could almost distinguish between HC and PC at the individual level, except for some outliers. The same individual differences were also visible in the theta/alpha ratio averaged across the whole head (fig. 5). The ROC-curve (appendix B.2) showed a cut-off value of 0.94, whereby chronic pain patients were detected with a sensitivity of 76% and a specificity of 91%.

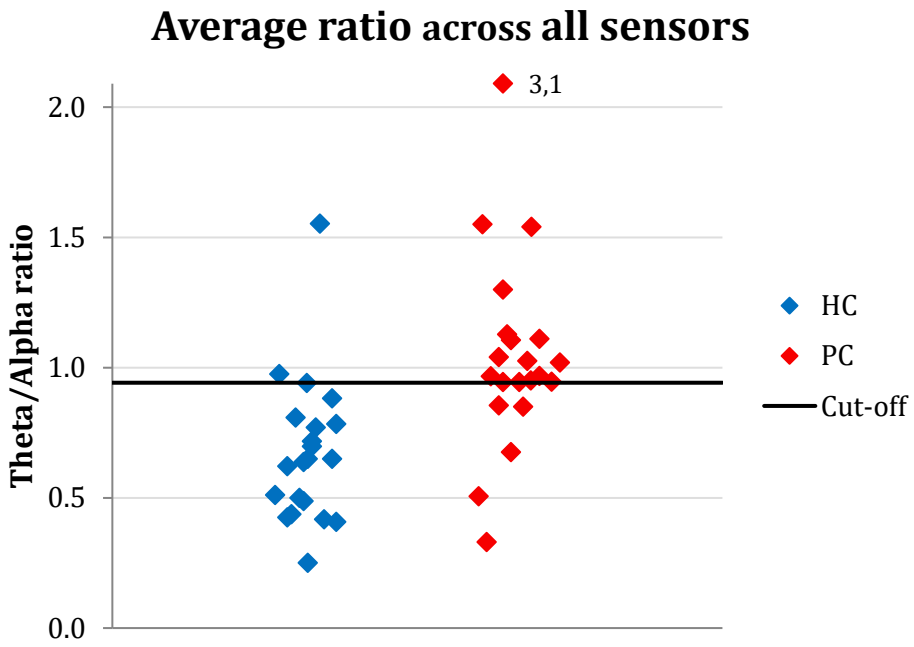

Figure 5: The average ratio across all sensor for each subject. Subjects in the healthy control (HC) group are shown in blue and subjects in the pain control (PC) group are shown in red. The black line indicates the cut-off value (determined with a ROC curve) to distinguish between HC and PC.

4.1.2 Alpha power distribution: source level

The differences between the two groups at source level are shown in figure 6. Sources which lighted up blue, showed a significantly higher theta/alpha ratio for the PC group ($p < 0.01$). The areas which showed the largest differences, were the insula (primarily the right insula), the cingulate cortex and the right temporal/occipital cortex.

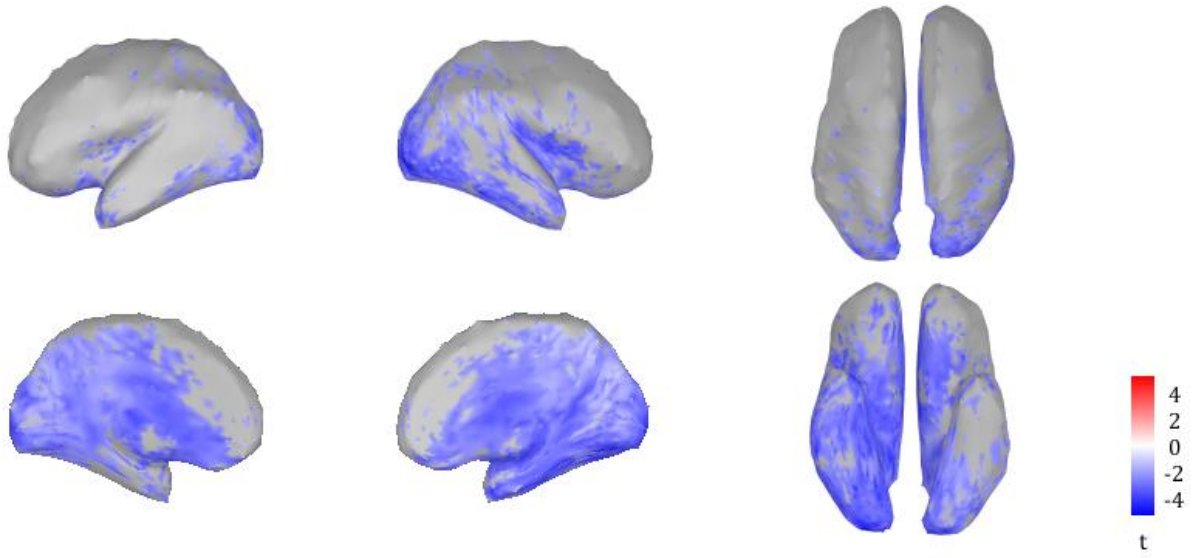

Figure 6: The results for a permutation t-test between the average (source level) theta/alpha ratios for the healthy controls and the average (source level) theta/alpha ratios for the pain controls. The results were false discovery rate (FDR) corrected for the number of sources. The values represented in the figure are t-values based on a significance level of $p < 0.01$. The areas which showed the largest differences between the two groups, were the insula (primarily the right insula), the cingulate cortex and the right temporal/occipital cortex.

4.1.3 Specific brain areas

The selected ROIs all showed a higher theta/alpha ratio for the PC group, compared to the HC group (fig. 7). The ROIs in the figure are sorted by the p-values for the difference in ratio between the two groups (p-values obtained through the permutation t-test, FDR corrected for the number of ROIs): the ROI with the lowest p-value is shown on the left and the ROI with the highest p-value is shown on the right. The right anterior insula, the right posterior S2, the right anterior S2, the posterior dorsal CC, the mid-posterior CC and the right posterior insula showed significantly higher ratios for the PC group ($p < 0.01$).

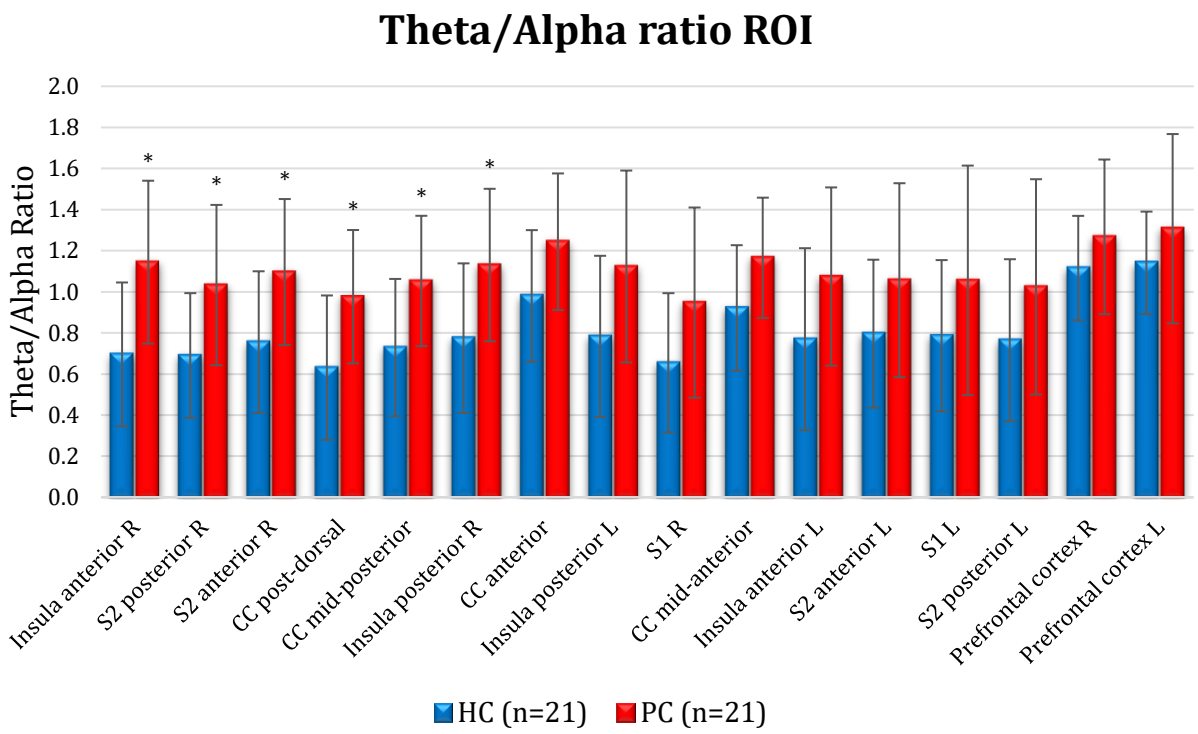

Figure 7: The average theta/alpha ratio in each region of interest (ROI) for the two groups, the error bars represent the standard deviation. The healthy controls (HC) are shown in blue and the pain controls (PC) are shown in red. The ROI with the most significant difference is shown on the left and the ROI with the least significant difference is shown on the right (p values were obtained by performing the permutation t-test). L = left, R = right, CC = cingulate cortex, S1 = primary somatosensory cortex, S2 = secondary somatosensory cortex, * = $p < 0.01$.

The connectivity matrices (correlation and coherence) for the differences between the HC and the PC for each ROI are shown in figure 8. The correlation values between the ROIs were generally low for both, the HC and the PC (appendix C.1) and therefore the differences between those two groups were only small. This is shown in figure 8 (left): a positive value means that the correlation or coherence between the two ROIs was larger for the HC and a negative value means that the correlation or coherence between the two ROIs was larger for the PC. The largest difference in correlation between the two groups was about 0.3 and found between the right S1 and the left S1: the correlation between those areas is larger for the PC than for the HC.

The coherence values between the ROIs showed a more distinct difference in connectivity between the two groups than the correlation values. The difference in coherence for the high theta band (7-9 Hz) and the low alpha band (9-11 Hz) show a similar connectivity pattern between the ROIs, however the coherence values were higher for the high theta band (appendix C.2). The largest difference in coherence (fig 8, right) between the two groups for the high theta band was found between the right anterior S2 and the right anterior insula: the coherence between those areas was about 0.5 for the PC and about 0.1 for the HC (appendix C.3). In the theta frequency band, there were also clear differences in coherence between the two groups for the different ROIs within the cingulate cortex and for the cingulate cortex and the S1: the coherence values between those areas were higher for the PC than for the HC.

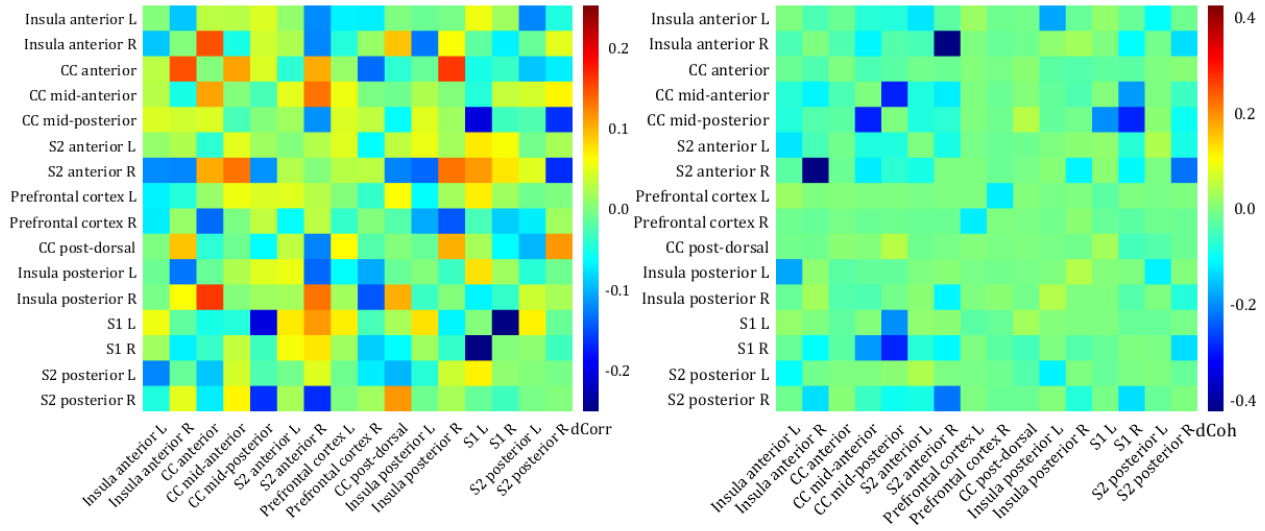

Figure 8: The differences in connectivity between the two groups, with (left) the difference between the correlation (within the regions of interest) of the healthy controls (HC) and the pain controls (PC) and (right) the difference between the coherence of the HC and the PC for the high theta band (7-9 Hz). The values are difference in correlation (left) or coherence (right) between the HC and PC, a positive value means a higher correlation/coherence between the two ROIs for the HC and a negative value means a higher correlation/coherence between the two ROIs for the PC. Note that the colorbars are scaled differently for the two matrices. L = left, R = right, CC = cingulate cortex, S1 = primary somatosensory cortex, S2 = secondary somatosensory cortex.

4.2 Spinal cord stimulation

For the PT group, 9 subjects (3 females) were included. The mean age for this group was 54 ± 10 years old. The mean reported NRS was 4.1 ± 3.0 after one week of tonic stimulation, 3.9 ± 2.1 after one week of burst stimulation and 5.4 ± 2.4 after one week of placebo stimulation. Five of the patients suffered from pain on their right side of the body, three on their left side and 1 suffered from pain on both sides.

4.2.1 Alpha power distribution: sensor level

The theta/alpha ratio topographies for the different stimulation modes are shown in figure 9. From left to right these are average ratios after one week of tonic stimulation, one week of burst stimulation and one week of placebo stimulation. Burst stimulation seems to show slightly lower ratios in the frontal area than the other two settings.

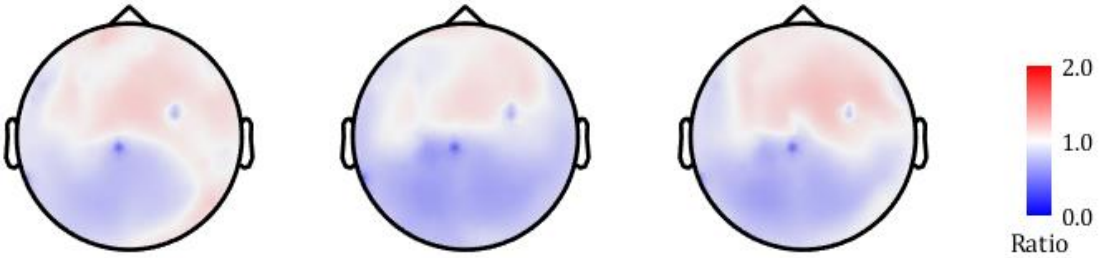

Figure 9: The average theta/alpha topographies (from left to right) after one week of tonic stimulation, one week of burst stimulation and one week of placebo stimulation.

The individual theta/alpha ratios averaged across the whole head seemed to be distributed similarly for each of the three settings (appendix D). The whole-head ratio averaged over the 9 subjects showed a ratio of 0.97 ± 0.30 for tonic stimulation, 0.88 ± 0.21 for burst stimulation and 0.94 ± 0.26 for placebo stimulation.

4.2.2 Alpha power distribution: source level

The differences in theta/alpha ratio between tonic stimulation and burst stimulation at source level are shown in figure 10. A positive difference (red) means a higher ratio during tonic stimulation and a negative difference (blue) means a higher ratio during burst stimulation. Especially the right temporal and occipital areas, but also the insula showed a higher ratio during tonic stimulation. The largest difference was seen in a small left frontal area, where the ratio was higher during tonic stimulation.

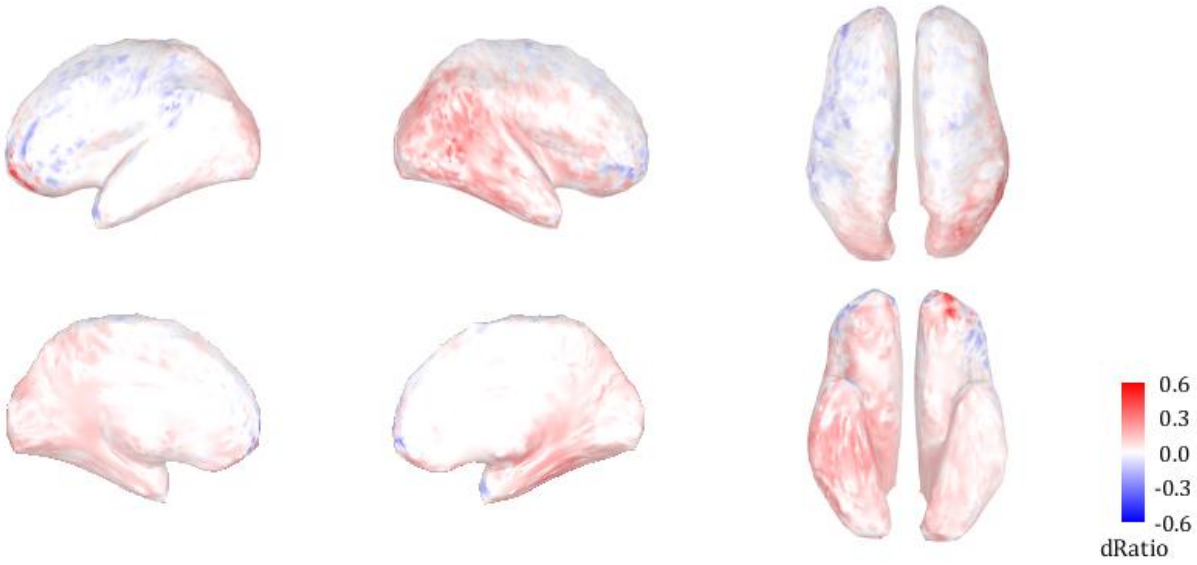

Figure 10: The difference in theta/alpha ratio (source level) between tonic stimulation and burst stimulation. A positive difference indicates a higher ratio during tonic stimulation and a negative difference indicates a higher ratio during burst stimulation.

The differences in theta/alpha ratio between tonic stimulation and placebo stimulation are shown in appendix E.1. The largest (positive) difference was again observed in the frontal area of the left hemisphere, where the ratio was higher during tonic stimulation. The differences in theta/alpha ratio between burst stimulation and placebo stimulation (appendix E.2) did not reveal one specific area with a larger difference than other areas. Overall, the ratio was higher for placebo stimulation compared to burst stimulation, whereby the right hemisphere showed this difference more clearly than the left hemisphere.

4.2.3 Specific frequency bands

The comparison of the specific frequency bands (theta, alpha1, alpha2, beta1, beta2 and beta3) between the three different stimulation settings revealed the largest differences in the alpha1 band (8-10 Hz) and the beta1 band (13-18 Hz) when comparing tonic stimulation to burst stimulation. The somatosensory cortex and the parietal lobe showed increased alpha1 power during tonic stimulation, compared to burst stimulation (fig 11). The difference in alpha1 power was maximally 0.04 (unitless), which represented about 10% difference between the two settings, as the maximum alpha1 power for both tonic and burst stimulation was about 0.3 (appendix F.1). The effect of increased alpha1 power was also visible when comparing tonic stimulation to placebo stimulation, but not when comparing burst stimulation to placebo stimulation (appendix F.2).

On the contrary, the power in the beta1 band for the somatosensory cortex and the parietal lobe was higher during burst stimulation, compared to tonic stimulation (fig 12). Although the figures showed the same scales, the difference in beta1 power was larger than the difference in alpha1 power: the maximum power for both tonic and burst stimulation was about 0.15 (unitless), therefore the value of 0.04 represented about 25% difference between the two settings. When comparing burst stimulation to placebo stimulation, the beta1 power for these same areas was also higher, but the comparison between tonic and placebo stimulation did not reveal a clear difference (appendix F.3). Note however that these differences are between the means of 9 subjects, the individual results varied as did the effect of the three stimulation settings on their pain perception.

A small area in the prefrontal cortex showed more theta power during tonic stimulation, compared to burst stimulation (appendix F.4). This increase in theta power was also reflected by an increased theta/alpha ratio during tonic stimulation in the same area (section 4.2.2). The difference was also visible between tonic and placebo stimulation, but not between burst and placebo stimulation.

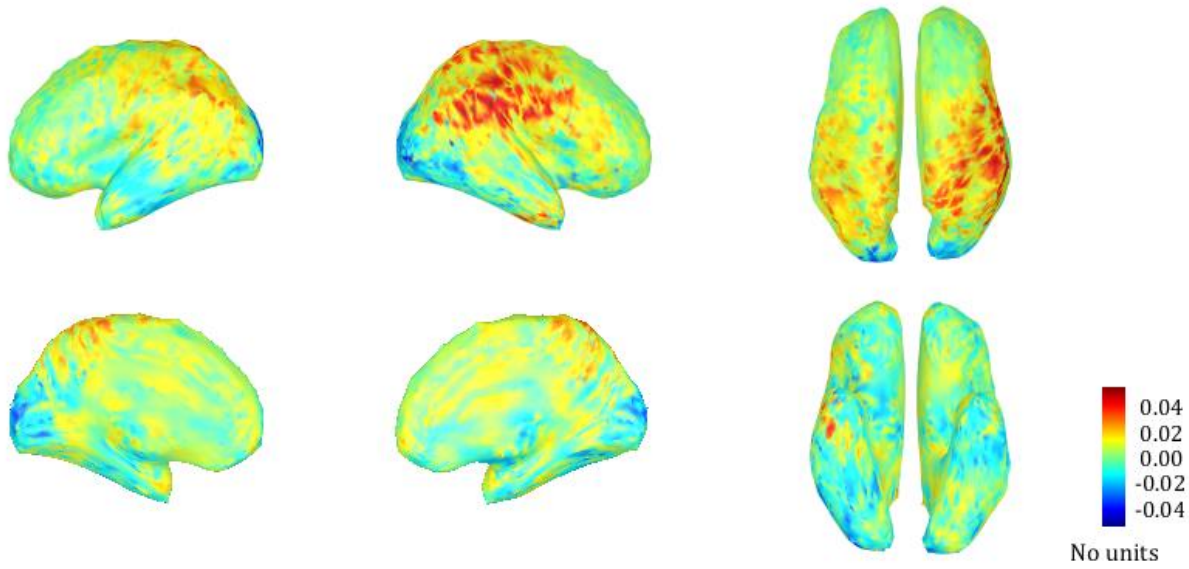

Figure 11: The difference in mean relative power in the alpha1 frequency band (8-10 Hz) between tonic stimulation and burst stimulation for every source. The positive values indicate more power in the alpha1 band during tonic stimulation, compared to burst stimulation. Especially the right hemisphere shows more alpha1 power in the somatosensory cortex and the parietal lobe during tonic stimulation.

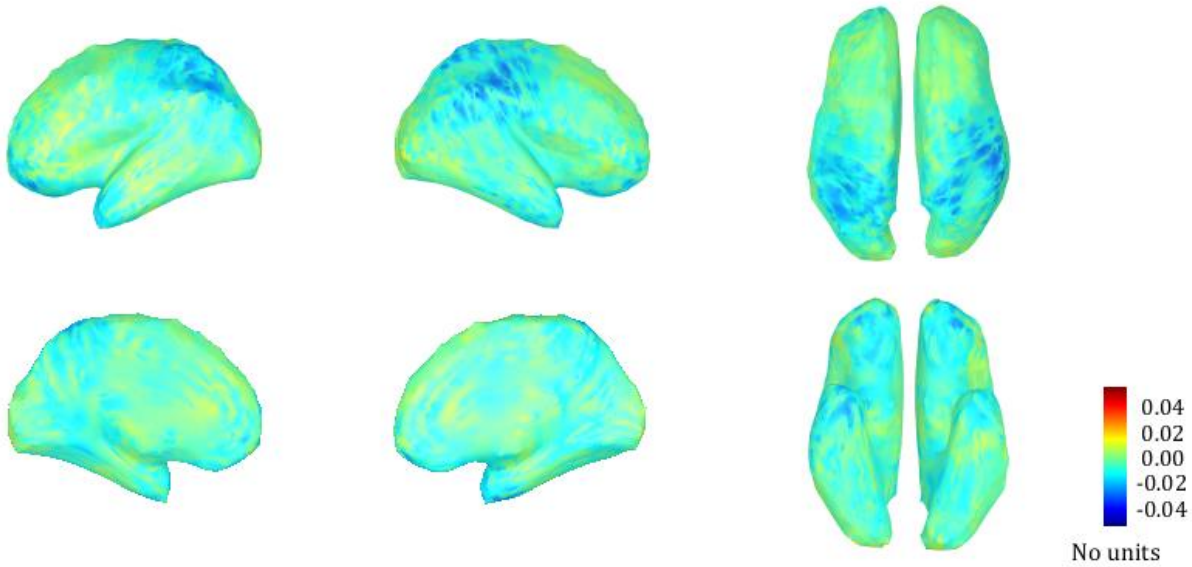

Figure 12: The difference in mean relative power in the beta1 frequency band (13-18 Hz) between tonic stimulation and burst stimulation for every source. The negative values indicate more power in the beta1 band during burst stimulation, compared to tonic stimulation. The somatosensory cortex and the parietal lobe show increased beta1 power during burst stimulation.

Chapter 5: Discussion

5.1 Main findings

Comparing between chronic pain patients and healthy, pain-free control subjects, we found that the alpha power distribution is significantly different between the two groups: the chronic pain patients showed higher theta/alpha ratios for several brain areas, indicative for slowing of the alpha frequencies. In the regions of interest, this difference in alpha power distribution was mainly observed in the right insula, the mid-posterior and posterior cingulate cortex and the right secondary somatosensory cortex. The coherence for the high theta frequencies between the right anterior insula and the right anterior S2 was much larger in the PC group, compared to the HC group. The comparison between tonic and burst stimulation showed a higher theta/alpha ratio during tonic stimulation for the temporal/occipital areas and the right insula. Furthermore, there were differences in power in the alpha1 and beta1 frequency bands in the somatosensory cortex and the parietal lobe between tonic and burst stimulation.

5.2 Thalamocortical dysrhythmia

5.2.1 Pain vs no pain

The theta/alpha ratio was significantly higher in PC group, compared to HC group. This higher ratio indicates that the peak in alpha frequencies is shifted towards the (lower) theta frequencies in patients with chronic pain. The increased ratio could also be caused by an increased power in theta frequencies, which has been reported in other literature. In a review about EEG patterns in chronic pain by Pinheiro et al, four of the six studies found an increased theta frequency power for the chronic pain subjects [20]. The increased theta power could be the result of a decreased inhibition of the thalamus. The slower theta waves reduce the lateral inhibition, which could cause increased gamma activity in the areas that surround the areas which show an increased theta activity. This is called thalamocortical dysrhythmia (TCD) and has been associated with multiple neurological and psychiatric disorders, amongst which chronic pain [17, 20, 22-24]. The theta/alpha ratio might reflect this phenomenon in our chronic pain patients as well.

In our source model, the increase in theta/alpha ratio seemed to originate from sources deeper than the cortex and spread into multiple cortical areas. We expected that this source could very well be the thalamus and to test this hypothesis, we incorporated the thalamus into our original source model (appendix E.3). That extended model indeed projected a vast part of the increased theta/alpha ratio in the thalamus. However, caution has to be taken when interpreting this finding, as more research is needed to confirm that MEG is indeed capable of detecting signals which originate in the thalamus [46]. Nevertheless, these results and the previous findings in literature, strongly suggest an alteration in thalamic behavior because of chronic pain.

Both, at sensor level and at source level, we saw the largest differences in theta/alpha ratio in the right hemisphere. This could be caused by the fact that a large part of our subjects (33%) suffered from chronic pain exclusively on their left side, and not the right side of their body, but it could also mean that the right hemisphere is more involved in the processing of pain than in the left

hemisphere. This has also been reported in literature: Pauli et al. found that pain sensitivity was associated with an increased right hemispheric activity [47] and Lugo et al. suggested that pain intensity perception is lateralized to the right hemisphere [48]. Also, the right insula is known to play a more significant role in attentional processes than the left insula [3, 49]. Another explanation for the larger differences in theta/alpha ratio on the right side is that TCD is mainly visible in the right hemisphere.

The average theta/alpha ratio across the whole head seemed to be able to distinguish quite accurately between the HC and PC. Especially the specificity (91%) was high for this method; most HC were correctly classified. The PC however showed a larger variation causing a sensitivity of 76%. The cut-off value could be decreased to obtain a larger sensitivity, as we could argue that the sensitivity is more important. Also, there are some clear outliers; the overall ratio of 3.1 for example, is clearly deviant from the other values and therefore has a larger impact on the cut-off value. Possibly, an explanation for the outliers can be found in the questionnaires (for example pain duration or peak pain intensity). The results from the questionnaires, but also the results from the other measures described in this thesis, could be incorporated in a more advanced model to improve the classifier. For this, a larger number of subjects would be desirable as well.

5.2.2 Spinal cord stimulation

The theta/alpha ratios at sensor level were slightly lower during burst SCS than during tonic or placebo stimulation. Also, the difference in theta/alpha ratio at source level between tonic and burst stimulation looks similar to the difference between chronic pain patients and healthy controls, except for the cingulate cortex (the CC shows comparable ratios for tonic and burst stimulation). Apart from the finding in the cingulate cortex, this could suggest that tonic stimulation does not affect TCD, but burst stimulation does or does to a larger extent. This might also be reflected in the pain scores; after one week of burst stimulation, the patients indicated lower pain scores on average. However, the differences in theta/alpha ratio and in the pain scores between the different stimulation settings were only small and there was variation between the subjects. With a larger number of subjects in the PT group, we would be able to group responders and non-responders to a certain stimulation setting, after which we expect to see clearer differences.

Moens et al. showed in a fMRI study that brief periods of SCS (during the trial stimulation phase) resulted in bilateral deactivation of the medial thalamus and the anterior and posterior CC. Ipsilateral (to the stimulation site) deactivation was found in the dorsal premotor cortex, the anterior part of the insula, the lentiform nucleus, the caudate nucleus, the S1 and the S2. Contralateral deactivation was found in the hypothalamus, the insula, the S2, the proprioceptive cortex, the visual cortex and the parahippocampal gyrus [50]. Stančák et al. found, with fMRI, that SCS (also during the trial stimulation phase) activated the primary motor cortex, the ipsilateral S2 and the contralateral posterior insula. When comparing periods with SCS to resting periods (no SCS), they saw decreased deactivation of the primary motor cortex, and the left postcentral gyrus [51]. With a larger number of subjects in the PT group, we can make a source model (preferably including the thalamus) and perform statistical analysis. Based on the described literature, we expect to find activity changes (compared to the PC) in the group with good responders to SCS for

the thalamus, the primary motor cortex, the CC, the S1 and S2 and the insula. Apart from the motor cortex, these same areas also showed an increased theta/alpha ratio (the S1 to a lesser extent) when comparing our PC to HC.

The cingulate cortex, specifically the anterior cingulate cortex, has also been a target for cortex stimulation [52]. Boccard et al. performed deep brain stimulation (DBS) in the ACC for 16 neuropathic pain patients, of which 11 subjects were included for analysis. They showed an overall improvement of visual analogue scale (VAS) scores [53]. Also, Spooner et al. presented a case study whereby they implanted DBS in a patient with neuropathic pain, they also reported better pain control after implantation [54]. Another form of cortex stimulation as a treatment of chronic pain is motor cortex stimulation (MCS). Although the precise working mechanism of MCS is unclear, MCS is believed to modulate pathologic hyperactivity of thalamic relay nuclei. The success rates for MCS were higher for facial pain (68%) than for central pain (54%) [55]. This literature shows that modulation of pain processing areas such as the motor cortex and the ACC is able to reduce pain in some chronic pain patients. Possibly, SCS works also through modulation of these (or other pain processing) brain areas, but by activating or deactivating the pain processing pathways through the spinal cord.

5.3 Connectivity measures

Differences in connectivity between the HC and the PC were mainly found in the coherence. The maximum coherence was found for the frequencies below 1.5 Hz. Since a large part of the PC had artifacts below 1 Hz, a 1 Hz high pass filter was applied for these subjects. Therefore, the coherence below 1 Hz is not expected to be reliable. The frequency band that showed the highest coherence after the frequencies below 1.5 Hz, was the high theta frequency band (7-9 Hz). Since this frequency band and the low alpha frequency band (9-11 Hz) were the main frequencies of interest, only these frequency bands were shown. The frequency resolution that was used for the coherence matrices (0.6 Hz) was different from the frequency resolution that was used for the other measures (0.25 Hz, for the alpha power distribution and the specific frequency bands). The reason for this was to reduce the computational effort; a higher frequency resolution caused the process to reach out of memory. A higher frequency resolution would however be desirable, since the width of the frequency bands of interest was only 2 Hz.

The areas that showed the highest difference in coherence for the high theta band between the HC and the PC were the right anterior S2 and the right anterior insula. Also, the ROI within the CC, and the CC and S1 showed a higher coherence for the PC in the high theta band. These areas are all located closely to each other, therefore a higher connectivity could be expected. Since the power in the high theta band was higher for the PC (they had a higher theta/alpha ratio), the connectivity in this frequency band could also be higher for the PC. However, the difference between the two groups for the high theta band was very large for the right anterior insula and the right anterior S2 (±0.1 for the HC and ±0.5 for the PC). Also for the low alpha band, the coherence between those ROIs was still larger for the PC and changes in connectivity for these ROIs in chronic pain patients have also been reported in literature.

Several studies have shown that the insula is involved in the processing of pain (amongst other psychological functions), specifically the affective/motivational component of pain [56, 57]. The insula has for example been mentioned for its involvement in pain processing for patients with fibromyalgia (FM): Hsiao et al. reported a decreased connectivity between the bilateral insula and the default mode network (DMN) for FM patients [58], Choe et al. reported a decreased connectivity within the DMN for FM patients [59] and Ichesco et al. reported an increased connectivity between the right insula and the CC for FM patients, but an increased connectivity between the left insula and the CC for controls [60]. So, there is literature which also shows an increased connectivity between the right insula and the other brain areas (involved in the processing of pain) for chronic pain patients, but there is also literature which suggests the opposite: that connectivity is decreased for chronic pain patients. Because the exact relation of the insula with other pain processing areas is still debated, this area and its connectivity with other ROI should be further explored with other connectivity measures.

We only found a difference in connectivity for the right insula, not for the left insula. Besides the study of Ichesco at al., there are other studies that have reported that the right insula is more important in the processing of pain than the left insula [3, 49, 60]. For example, Cauda et al. also found a stronger connectivity between the right insula and the areas associated with attentional processes (such as the ACC and the thalamus) than the left insula. Our findings and the literature suggest that the right insula is more important in the processing of pain than the left insula.

The correlation values showed very little difference between the two groups. Although both measures (correlation and coherence) were used to describe a relation between ROIs, the correlation values indicate a relation between areas in the time domain, where the coherence values indicate a relation between areas in the frequency domain. The correlation was computed with the assumption that the time lag between two ROIs was 0. This might not be entirely accurate, because the distance between two ROIs might cause a small lag in response. Also, the correlation values were averaged across the five-minute recordings, negative correlation values might have cancelled out positive correlation values, resulting in lower values than the coherence values. In order to reduce these effects, I also computed the maximum correlation across the five-minute recordings (appendix C.4). This however did not show larger differences than the mean correlations did. In addition, taking the maximum coherence across five minutes, is more sensitive to sudden non-physiological changes in the time signal. Because of these disadvantages, the correlation might therefore be a suboptimal measure for describing the connectivity in this case.

5.4 Specific frequency bands

De Ridder et al. suggested that burst stimulation works through the lateral and medial pathway, but tonic stimulation only though the lateral pathway. Therefore, we expected to find the biggest differences in the ACC, the somatosensory and insular cortices, when comparing cortical activity during tonic and burst stimulation [5, 9]: the ACC and the anterior insula were expected to be more active during burst stimulation and the somatosensory cortex was expected to be more active during tonic stimulation. The somatosensory cortex indeed showed slightly more activity in the alpha1 band for tonic stimulation, however we did not find increased activity in the ACC and insula

during burst stimulation (in none of the frequency bands). The alpha1 power increase in the somatosensory cortex during tonic stimulation could be the result of the paresthesia, caused by tonic stimulation. This explanation was further supported after comparing tonic and placebo stimulation, and burst and placebo stimulation. The difference was also visible between tonic and placebo, but not between burst and placebo (where neither of the two causes paresthesia). Overall, our results do not show such a clear difference between tonic and burst stimulation to suggest that the two stimulation modes work through different pathways. It seems more likely that both, the tonic and the burst stimulation work through the concept of the gate control theory: the large Aβ-fibers block the pain signals of the smaller Aδ and C-fibers but cause perceived sensations, whereas burst stimulation modulates the Aβ-fibers below the paresthesia threshold [9].

When comparing tonic stimulation and burst stimulation, a difference was also found in the beta1 frequency band, again for the somatosensory cortex. Although alpha1 power was higher during tonic stimulation in this area, beta1 power was higher during burst stimulation. The comparison between tonic and placebo stimulation did not reveal clear differences in beta1 activity, indicating that the beta1 power is increased during burst stimulation only. This suggests that both SCS settings are processed in the somatosensory cortex, whereby tonic stimulation causes alpha1 oscillations and burst stimulation causes beta1 oscillations. However, we do not have an explanation for this yet and further analysis with a larger number of subjects is needed to explore this finding.

The prefrontal cortex showed an increased theta power when comparing tonic to burst stimulation. As this difference was also visible between tonic and placebo, but not during burst and placebo, this difference could be caused by the tonic stimulation. This increased theta power was also reflected in the theta/alpha ratio; the ratio was higher for a small area of the prefrontal cortex when comparing tonic versus burst stimulation. Although other areas of the prefrontal cortex (such as the dorsolateral prefrontal cortex) have been reported to be involved in the processing of pain [9, 20], this small prefrontal area has not been reported yet in association with chronic pain. The data has been cleaned of eye blinks, but the location and the frequency of this difference could also originate from remaining eye movements. The source models of the individual subjects revealed that the theta power in the prefrontal cortex was higher during tonic stimulation (compared to burst) in three of the nine subjects. These three subjects might have had more eye movements during the recording, but it is unlikely that they only showed more eye movements during tonic stimulation, and less during burst stimulation. A larger number of subjects and extended data analysis is necessary to further explore this finding.

5.5 Considerations

5.5.1 Measure for alpha power distribution

The same measure as described by Schulman et al. [17] was used for looking at the alpha power distribution. The goal of this measure is to indicate whether the power of the dominant frequency peak, generally the alpha peak, is shifted towards the theta frequency for chronic pain patients, which could be indicative for TCD. The theta/alpha ratio however, only divides the power for the frequencies 7-9 Hz by the power for the frequencies 9-11 Hz. For most of our subjects, we saw a

very clear dominant frequency, wherefore a possible shift could be captured accurately, due to the shape of the peak. This is visualized in a schematic representation (fig 13): each line represents a PSD, with a different dominant frequency. The green line has a peak around 8 Hz, which is within the boundaries of the theta/alpha ratio. Although the blue line has its dominant peak around 12.5 Hz, the ratio still gives a good indication about the location of the peak. For two of our subjects however (both in the PC group), the frequency of the dominant peak was even higher, or the peak was less clear. This caused the theta/alpha ratio to be less accurate, as the lower frequencies, with a higher power than the theta frequencies, caused an increased ratio although the actual peak was not shifted (as is the case for the red line in fig 13).

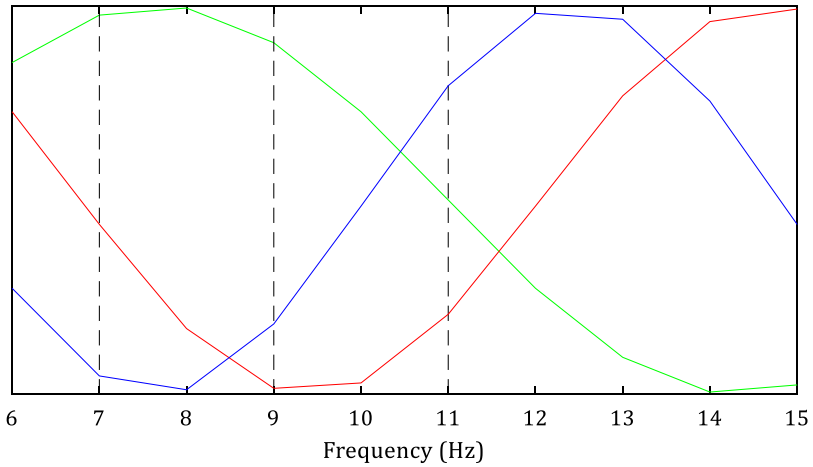

Figure 13: A schematic representation of the working mechanism of the theta/alpha ratio. The three lines represent power spectral densities with different frequencies for their dominant peak. The theta/alpha ratio accurately describes the frequency of the dominant peak for the green line and the blue line. For the red line however, the frequency of the dominant peak is too high, causing an increased ratio, although the alpha peak is not shifted towards theta frequencies.

There are also other ways to study changes in the alpha frequency band. For example, we could examine the alpha power distribution by looking at the alpha peak; the frequency where the alpha power is highest. An example of such a method is the center of gravity (CoG) method [61]. The CoG is computed within a predefined frequency band: the average frequency weighted by amplitude is divided by the sum of amplitudes:

$$CoG = \frac{\sum_{i=1}^{n} f_i * a_i}{\sum_{i=1}^{n} a_i}$$

I also tested this method for a small number of subjects, to compare with the theta/alpha ratio. To also capture the peaks of the two subjects with a higher frequency, the frequency band that was used for the CoG method was chosen to be 7-13 Hz. The CoG method indeed described the location of the peak more accurately for the two subjects with a higher alpha peak frequency, but for some of the other subjects, it was less accurate. For example, when the alpha peak consisted of two peaks, the peak was placed in between the two peaks with the CoG method. However, the first peak (with lower frequency than the second peak) generally has a lower power than the second peak, wherefore the dominant frequency can be assumed to be the second peak. The distribution of power was captured more accurately with the theta/alpha ratio than the CoG method and the theta/alpha ratio was less accurate for only two subjects. Therefore, the theta/alpha ratio was chosen for further analysis.

5.5.2 Confounders

There are several confounders that could have affected our results. An example of such a confounder is medication; most of our subjects in the PC group and the PT group used medication for their pain. This medication could also have caused the differences that we observed between the groups. Malver et al. reviewed the effects of analgesics on spontaneous EEG and found that analgesics primarily cause an increased activity in the delta band. Although a few studies reported that the spontaneous theta and alpha frequencies are affected by analgesics, the results of these studies are varying (some show an increased activity, some show a decreased activity) [62].

Another confounder might have been the age of the subjects. Age is known to affect the frequency of the dominant brain rhythm: although the frequency remains relatively stable after the age of 20, there is a slow decline in frequency with increasing age [63]. The mean age for the HC group and the PC group was very similar, but the subjects in the PT group were slightly older. Therefore, the PTs might show a slower rhythm as a result of aging. However, since the HC and PC were of similar age and showed clear differences, we expect the influence of age to be minimal.

Also, anxiety and depression often accompany chronic pain. For example, psychiatric disorders have also been related to TCD and could therefore also affect the theta/alpha ratio [20]. Depression is known to influence the insula, which is also involved in the affective-motivational dimension of pain. The brain areas involved in the sensory dimension of pain (mainly the somatosensory cortex) however, are not related to depression [56, 57]. However, there are EEG studies that have shown a reduced alpha power in the right anterior hemisphere and increased alpha power in right parietemporal areas for subjects with depression [64, 65]. Also, other studies reported an increased theta power in the right anterior hemisphere, whereby source localization revealed involvement of parts of the ACC [65]. Since these frequency changes could also be reflected by the theta/alpha ratio, it is important to further investigate the effect of depression on our measures. Therefore, we will include the results for the HADS questionnaires in the classification of our subjects.

5.5.3 SCS settings

The subjects in the PT group were recorded after one-week evaluation periods of tonic, burst and placebo stimulation. The placebo stimulation however, was the lowest possible intensity (0.05 mA, 2 pulses with a pulse width of 100 μs) of burst stimulation. This is different from the study of de Ridder et al. [5, 9], where the SCS was turned completely off for placebo. We do not expect any functional effect of our placebo stimulation, as the intensity of placebo stimulation was very low. This was also reflected by the higher pain scores that our subjects indicated after one week of our placebo stimulation. However, we cannot rule out that there were no effects at all, since the stimulation was not completely turned off.

The stimulation that the PTs had received before the start of this study varied as well. They had received SCS, either tonic or burst, for at least three months, but there are also subjects who had received SCS for multiple years. The long-term effect of SCS on the cortical activity has not been studied yet, but the duration that patients have received SCS might cause differences in cortical activity. Also, it is possible that the effect of tonic or burst stimulation on cortical activity is still

present after the stimulation settings were switched and that these effects were still present after for example one week of placebo stimulation.

5.5.4 Individual anatomy

For an accurate estimation of the cortical surface, for some subjects their individual MRI was used. However, not for every subject an MRI was available, especially not for the subjects with a spinal cord stimulator (which is in many cases not yet MRI compatible). To still make a plausible estimation of the cortical surface for every subject, the head shape was digitized with many points. Therefore, the default MRI could be warped to estimate an individual MRI and estimate an individual cortical surface. Although the warping of a default MRI is not as accurate as an individual MRI, the warping of a default MRI has shown to be a reliable approximation of an individual MRI [66].

The selection of ROI was however not equally accurate for each subject. As the Destrieux atlas did not fit the ROI perfectly, the vertices for the ROI were adapted manually using Brainstorm. The vertices were selected based on the default anatomy and subsequently projected on the subject's anatomy (either warped or individual MRI). Since the vertices were selected based on the default anatomy, the subjects with an individual MRI might have slightly different vertices for each ROI. The analysis for the ROI could have been more accurate with a better fitting atlas for the intended ROI, so that the vertices could be segmented using the FreeSurfer software. However, visual inspection of the ROI showed that the projection of the manually selected vertices approximated the intended ROI sufficiently.

5.5.5 Source model normalization

Several assumptions were made to construct the source models. The source models were constructed with constrained dipoles, mainly to reduce computation time. Using constrained dipoles is an often-used technique, as the main contributor of the MEG signal is believed to be the synchronized activity of cortical pyramidal neurons. As these neurons are also oriented approximately normal to the cortical surface, the dipoles could also be assumed oriented towards the cortical surface [15, 36]. For the forward model method, the simplified overlapping spheres method was used. Although there are also more sophisticated forward models, the overlapping spheres method has shown similar accuracy with much less computational costs and was therefore chosen [37]. Another choice was the use of dSPM for the normalization of the minimum norm estimates. Normalization is often used, because MNE tends to estimate higher values for the sources closer to the sensors. Also, the amplitude of the estimates depends on the signal to noise ratio, which makes it more difficult to interpret. Brainstorm offers three normalization methods: dSPM, sLORETA and a Z-score transformation. The dSPM method was used, because it corrects for the noise and for overestimating sources closer to the surface, and gives z-score similar values, which makes the source models easier to interpret for the individual results. For the group results however, subsequent statistical analysis was performed, wherefore non-normalized source maps might have been more accurate [67]. In order to test this, the source model with the thalamus was computed without the dSPM normalization. As the model with the thalamus showed similar results

(whereby only areas surrounding the thalamus showed different activity) and recomputing the source models would be very time consuming, the dSPM normalization was used for further analysis.

5.5.6 Statistical analysis

For the statistical analysis, a nonparametric permutation t-test was used, with FDR correction for the number of signals. This method is also implemented in Brainstorm and since the data was not normally distributed, the most suitable available method. This method was designed with the intention of a very large number of permutations, since there is a very large number of pairs (with the number of sensors, sources, timepoints, frequency points). To reduce computation time, a Monte Carlo approximation was used with only 1000 permutations. Although this is a commonly used approximation and a larger number of permutations would probably not give completely different results, a larger number of permutations would increase the accuracy of the test [43, 44]. For the alpha power distribution at sensor level, I also ran the permutation test with 10,000 permutations. As this resulted in similar differences, the number of 1000 permutations were used for the other measures.

5.6 Recommendations

The findings for the theta/alpha ratio suggest the that TCD plays an important role. In order to further explore this idea, further analysis of this data within the gamma frequency band would be useful. If TCD indeed plays a role, we would expect an increased gamma activity for the areas that surrounded the areas which showed a slowing of the dominant frequency. Also, it would be useful to further explore the thalamic source model. For example, connectivity measures (for theta frequencies) between the thalamus and the ROIs could confirm TCD. The thalamic source model might also give insight in the thalamic response to SCS and its possible differences between tonic and burst stimulation.

The connectivity was analyzed by calculating the correlation and the coherence. These are only two connectivity measures, and there are many other ways of looking at the connectivity. For further analysis, other connectivity measures (for example, phase synchronization indexes) could give more insights. The connectivity between the right anterior insula and the other (pain processing) brain areas would be a main area of interest.

Before any conclusions can be drawn about the working mechanisms of SCS and its different stimulation settings, more subjects with SCS are needed, preferably with very favorable effects of one of the stimulation settings and much less effect of the others. Then, we can also make a clearer distinction between responders and non-responders and further explore why some subjects do respond well to SCS and others do not. With a larger number of subjects in the PT group and a distinction between responders and non-responders, it will also be possible to analyze whether there is a change in connectivity as a result of SCS.

Conclusion

The theta/alpha ratios showed an overall slowing of the alpha frequencies for the chronic pain patients. This slowing of alpha frequencies was mainly observed in the right insula, the mid-posterior and posterior cingulate cortex and the right secondary somatosensory cortex. These findings suggested the involvement of thalamocortical dysrhythmia. In addition, the coherence between the right anterior insula and the right anterior S2 showed to be much larger in the PC group, suggesting an increased connectivity between the right anterior insula and the pain processing network for chronic pain patients.

As the comparison between tonic and burst SCS showed a higher theta/alpha ratio during tonic stimulation in the temporal/occipital areas and the right insula, burst stimulation seemed to reduce TCD to a larger extent than tonic stimulation. The analysis for the specific frequency bands did not give a clear reason to assume that burst stimulation works through different pathways than tonic stimulation. Modulation of the same pathways seems more likely, but the differences at cortical level will have to be explored further in a larger number of subjects, whereby the subjects can be grouped for responders and non-responders for each stimulation setting.

References

1. Merskey, H. and N. Bogduk, *Classification of chronic pain, IASP Task Force on Taxonomy.* 1994, IASP Press: Seattle. p. 210.
2. Price, D.D., *Psychological and neural mechanisms of the affective dimension of pain.* Science, 2000. **288**(5472): p. 1769-72.
3. Craig, A.D., *How do you feel? Interoception: the sense of the physiological condition of the body.* Nat Rev Neurosci, 2002. **3**(8): p. 655-66.
4. Iannetti, G.D. and A. Mouraux, *From the neuromatrix to the pain matrix (and back).* Exp Brain Res, 2010. **205**(1): p. 1-12.
5. De Ridder, D. and S. Vanneste, *Burst and Tonic Spinal Cord Stimulation: Different and Common Brain Mechanisms.* Neuromodulation, 2016. **19**(1): p. 47-59.
6. Felix, E.R., *Chronic neuropathic pain in SCI: evaluation and treatment.* Phys Med Rehabil Clin N Am, 2014. **25**(3): p. 545-71, viii.
7. Hussain, A. and M. Erdek, *Interventional pain management for failed back surgery syndrome.* Pain Pract, 2014. **14**(1): p. 64-78.
8. Melzack, R. and P.D. Wall, *Pain mechanisms: a new theory.* Science, 1965. **150**(3699): p. 971-9.
9. De Ridder, D., et al., *Burst spinal cord stimulation for limb and back pain.* World Neurosurg, 2013. **80**(5): p. 642-649.e1.
10. Zhang, T.C., J.J. Janik, and W.M. Grill, *Mechanisms and models of spinal cord stimulation for the treatment of neuropathic pain.* Brain Res, 2014. **1569**: p. 19-31.
11. de Vos, C.C., et al., *Burst spinal cord stimulation evaluated in patients with failed back surgery syndrome and painful diabetic neuropathy.* Neuromodulation, 2014. **17**(2): p. 152-9.
12. Hou, S., K. Kemp, and M. Grabois, *A Systematic Evaluation of Burst Spinal Cord Stimulation for Chronic Back and Limb Pain.* Neuromodulation, 2016. **19**(4): p. 398-405.
13. Van Buyten, J.P., et al., *High-frequency spinal cord stimulation for the treatment of chronic back pain patients: results of a prospective multicenter European clinical study.* Neuromodulation, 2013. **16**(1): p. 59-65; discussion 65-6.
14. Singh, S.P., *Magnetoencephalography: Basic principles.* Annals of Indian Academy of Neurology, 2014. **17**(Suppl 1): p. S107-S112.
15. Baillet, S., J.C. Mosher, and R.M. Leahy, *Electromagnetic brain mapping.* IEEE Signal Processing Magazine, 2001. **18**(6): p. 14-30.
16. Witjes, B., *M2 internship report: Neural Correlates of Spinal Cord Stimulation*. 2016, Medisch Spectrum Twente & University of Twente: Enschede.
17. Schulman, J.J., et al., *Thalamocortical dysrhythmia syndrome: MEG imaging of neuropathic pain.* Thalamus & Related Systems, 2005. **3**(1): p. 33-39.
18. Kumar, K., et al., *The effects of spinal cord stimulation in neuropathic pain are sustained: a 24-month follow-up of the prospective randomized controlled multicenter trial of the effectiveness of spinal cord stimulation.* Neurosurgery, 2008. **63**(4): p. 762-70; discussion 770.
19. de Vries, M., et al., *Altered resting state EEG in chronic pancreatitis patients: toward a marker for chronic pain.* Journal of Pain Research, 2013. **6**: p. 815-824.
20. Pinheiro, E.S., et al., *Electroencephalographic Patterns in Chronic Pain: A Systematic Review of the Literature.* PLoS One, 2016. **11**(2): p. e0149085.
21. Moseley, G.L. and H. Flor, *Targeting cortical representations in the treatment of chronic pain: a review.* Neurorehabil Neural Repair, 2012. **26**(6): p. 646-52.
22. Ploner, M., C. Sorg, and J. Gross, *Brain Rhythms of Pain.* Trends in Cognitive Sciences, 2017. **21**(2): p. 100-110.
23. Sarnthein, J. and D. Jeanmonod, *High thalamocortical theta coherence in patients with neurogenic pain.* Neuroimage, 2008. **39**(4): p. 1910-7.

24. Sarnthein, J., et al., *Increased EEG power and slowed dominant frequency in patients with neurogenic pain.* Brain, 2006. **129**(Pt 1): p. 55-64.
25. Fonseca, L.C., et al., *Comparison of quantitative EEG between patients with Alzheimer's disease and those with Parkinson's disease dementia.* Clinical Neurophysiology, 2013. **124**(10): p. 1970-1974.
26. Brainard, D.H., *The Psychophysics Toolbox.* Spat Vis, 1997. **10**(4): p. 433-6.
27. Pelli, D.G., *The VideoToolbox software for visual psychophysics: transforming numbers into movies.* Spat Vis, 1997. **10**(4): p. 437-42.
28. Rustamov, N., et al., *Inhibitory effects of heterotopic noxious counter-stimulation on perception and brain activity related to Abeta-fibre activation.* Eur J Neurosci, 2016. **44**(1): p. 1771-8.
29. Ladouceur, A., et al., *Top-down attentional modulation of analgesia induced by heterotopic noxious counterstimulation.* Pain, 2012. **153**(8): p. 1755-62.
30. Tadel, F., et al., *Brainstorm: a user-friendly application for MEG/EEG analysis.* Comput Intell Neurosci, 2011. **2011**: p. 879716.
31. Muthukumaraswamy, S.D., *High-frequency brain activity and muscle artifacts in MEG/EEG: a review and recommendations.* Frontiers in Human Neuroscience, 2013. **7**: p. 138.
32. Tesche, C.D., et al., *Signal-space projections of MEG data characterize both distributed and well-localized neuronal sources.* Electroencephalogr Clin Neurophysiol, 1995. **95**(3): p. 189-200.
33. Uusitalo, M.A. and R.J. Ilmoniemi, *Signal-space projection method for separating MEG or EEG into components.* Med Biol Eng Comput, 1997. **35**(2): p. 135-40.
34. Youden, W.J., *Index for rating diagnostic tests.* Cancer, 1950. **3**(1): p. 32-35.
35. Dale, A.M., B. Fischl, and M.I. Sereno, *Cortical surface-based analysis. I. Segmentation and surface reconstruction.* Neuroimage, 1999. **9**(2): p. 179-94.
36. Hämäläinen, M.S., *Overcoming Challenges of MEG/EEG Data Analysis: Insights from Biophysics, Anatomy, and Physiology.* 2013
37. Huang, M.X., J.C. Mosher, and R.M. Leahy, *A sensor-weighted overlapping-sphere head model and exhaustive head model comparison for MEG.* Phys Med Biol, 1999. **44**(2): p. 423-40.
38. Hamalainen, M.S. and R.J. Ilmoniemi, *Interpreting magnetic fields of the brain: minimum norm estimates.* Med Biol Eng Comput, 1994. **32**(1): p. 35-42.
39. Dale, A.M., et al., *Dynamic statistical parametric mapping: combining fMRI and MEG for high-resolution imaging of cortical activity.* Neuron, 2000. **26**(1): p. 55-67.
40. Fischl, B., et al., *Automatically Parcellating the Human Cerebral Cortex.* Cerebral Cortex, 2004. **14**(1): p. 11-22.
41. Destrieux, C., et al., *Automatic parcellation of human cortical gyri and sulci using standard anatomical nomenclature.* NeuroImage, 2010. **53**(1): p. 1-15.
42. Niso, G., et al., *HERMES: towards an integrated toolbox to characterize functional and effective brain connectivity.* Neuroinformatics, 2013. **11**(4): p. 405-34.
43. Pantazis, D., et al., *A comparison of random field theory and permutation methods for the statistical analysis of MEG data.* Neuroimage, 2005. **25**(2): p. 383-94.
44. Maris, E. and R. Oostenveld, *Nonparametric statistical testing of EEG- and MEG-data.* J Neurosci Methods, 2007. **164**(1): p. 177-90.
45. Benjamini, Y. and Y. Hochberg, *Controlling the False Discovery Rate: A Practical and Powerful Approach to Multiple Testing.* Journal of the Royal Statistical Society. Series B (Methodological), 1995. **57**(1): p. 289-300.
46. Attal, Y., et al., *Modeling and detecting deep brain activity with MEG & EEG.* Conf Proc IEEE Eng Med Biol Soc, 2007. **2007**: p. 4937-40.
47. Pauli, P., G. Wiedemann, and M. Nickola, *Pain sensitivity, cerebral laterality, and negative affect.* Pain, 1999. **80**(1-2): p. 359-64.

48. Lugo, M., et al., *Sensory lateralization in pain subjective perception for noxious heat stimulus.* Somatosens Mot Res, 2002. **19**(3): p. 207-12.
49. Cauda, F., et al., *Functional connectivity of the insula in the resting brain.* Neuroimage, 2011. **55**(1): p. 8-23.
50. Moens, M., et al., *Spinal cord stimulation modulates cerebral function: an fMRI study.* Neuroradiology, 2012. **54**(12): p. 1399-407.
51. Stancak, A., et al., *Functional magnetic resonance imaging of cerebral activation during spinal cord stimulation in failed back surgery syndrome patients.* Eur J Pain, 2008. **12**(2): p. 137-48.
52. Russo, J.F. and S.A. Sheth, *Deep brain stimulation of the dorsal anterior cingulate cortex for the treatment of chronic neuropathic pain.* Neurosurg Focus, 2015. **38**(6): p. E11.
53. Boccard, S.G., et al., *Targeting the affective component of chronic pain: a case series of deep brain stimulation of the anterior cingulate cortex.* Neurosurgery, 2014. **74**(6): p. 628-35; discussion 635-7.
54. John Spooner, et al., *Neuromodulation of the cingulum for neuropathic pain after spinal cord injury.* Journal of Neurosurgery, 2007. **107**(1): p. 169-172.
55. Ostergard, T., C. Munyon, and J.P. Miller, *Motor Cortex Stimulation for Chronic Pain.* Neurosurgery Clinics of North America, 2014. **25**(4): p. 693-698.
56. Mutschler, I., et al., *Pain and emotion in the insular cortex: evidence for functional reorganization in major depression.* Neurosci Lett, 2012. **520**(2): p. 204-9.
57. Giesecke, T., et al., *The relationship between depression, clinical pain, and experimental pain in a chronic pain cohort.* Arthritis Rheum, 2005. **52**(5): p. 1577-84.
58. Hsiao, F.J., et al., *Altered insula-default mode network connectivity in fibromyalgia: a resting-state magnetoencephalographic study.* J Headache Pain, 2017. **18**(1): p. 89.
59. Choe, M.K., et al., *Disrupted Resting State Network of Fibromyalgia in Theta frequency.* Sci Rep, 2018. **8**(1): p. 2064.
60. Ichesco, E., et al., *Altered resting state connectivity of the insular cortex in individuals with fibromyalgia.* J Pain, 2014. **15**(8): p. 815-826.e1.
61. Furman, A.J., et al., *Cerebral peak alpha frequency predicts individual differences in pain sensitivity.* Neuroimage, 2017. **167**: p. 203-210.
62. Malver, L.P., et al., *Electroencephalography and analgesics.* Br J Clin Pharmacol, 2014. **77**(1): p. 72-95.
63. Lodder, S.S. and M.J. van Putten, *Automated EEG analysis: characterizing the posterior dominant rhythm.* J Neurosci Methods, 2011. **200**(1): p. 86-93.
64. Ionescu, D.F., et al., *Neurobiology of anxious depression: a review.* Depress Anxiety, 2013. **30**(4): p. 374-85.
65. Jaworska, N. and A. Protzner, *Electrocortical features of depression and their clinical utility in assessing antidepressant treatment outcome.* Can J Psychiatry, 2013. **58**(9): p. 509-14.
66. Gohel, B., et al., *Approximate Subject Specific Pseudo MRI from an Available MRI Dataset for MEG Source Imaging.* Front Neuroinform, 2017. **11**: p. 50.
67. Tadel, F., et al. *Tutorial 22: Source estimation*. [cited 2018 30-08]; Available from: https://neuroimage.usc.edu/brainstorm/Tutorials/SourceEstimation.

Appendix

A Regions of interest

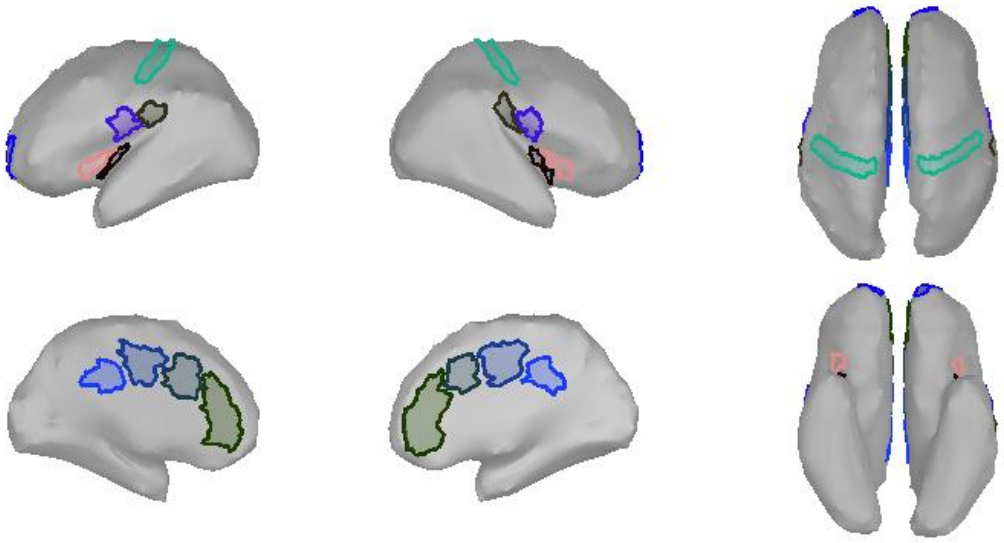

Figure 14: The vertices that were selected as a region of interest (ROI). The following ROIs were selected: The prefrontal cortex, the insular cortex (anterior and posterior), the primary somatosensory cortex, the secondary somatosensory cortex (anterior and posterior) and the cingulate cortex (anterior, mid-anterior, mid-posterior, posterior).

B.1 Alpha power distribution (sensor level): the individual topographies

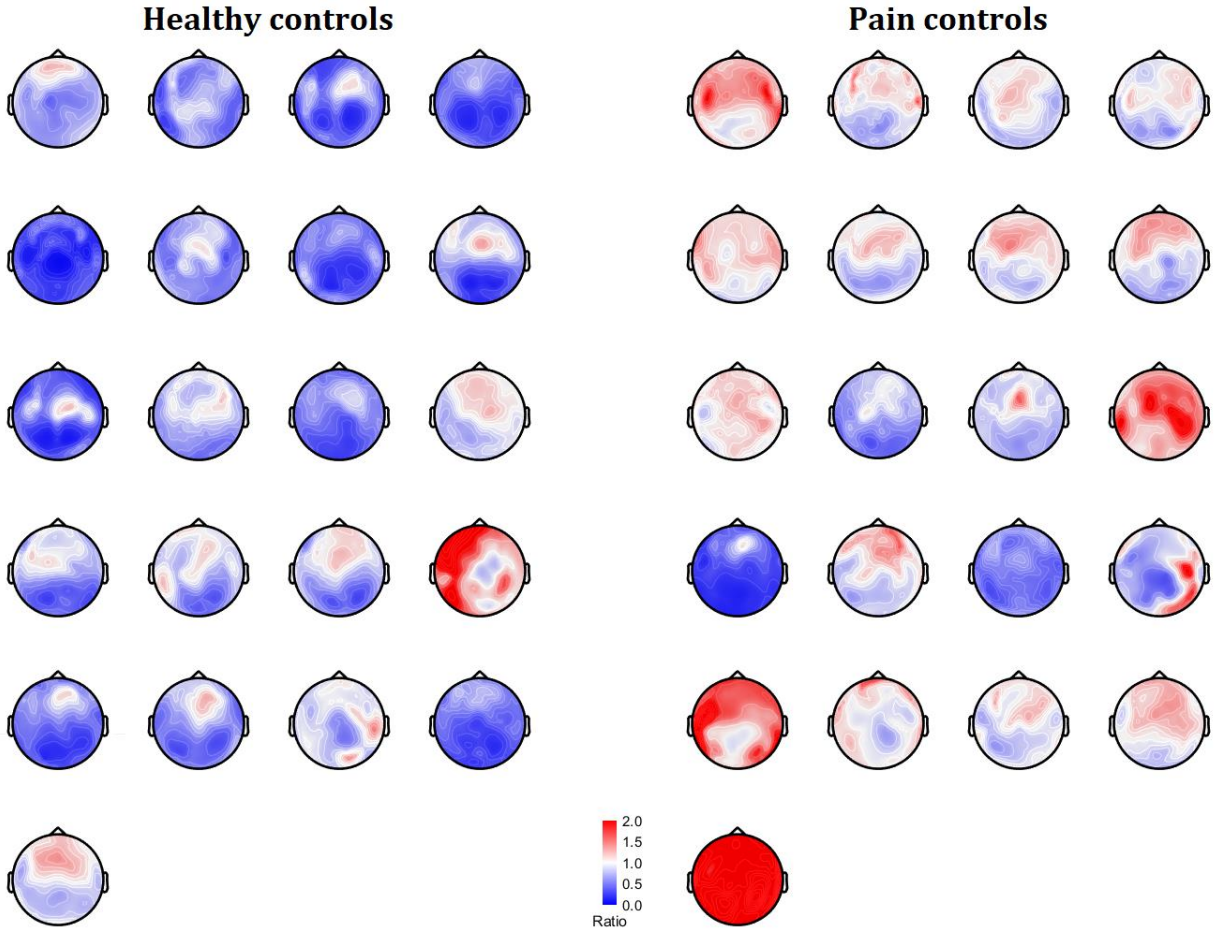

Figure 15: The individual theta/alpha ratio topographies for the healthy controls (HC, left) and the pain controls (PC, right). The theta/alpha ratios were determined by calculating the ratio between power in the theta frequency band (7-9 Hz) and the power in the alpha frequency band (9-11 Hz) for every MEG sensor.

B.2 Alpha power distribution (sensor level): ROC curve

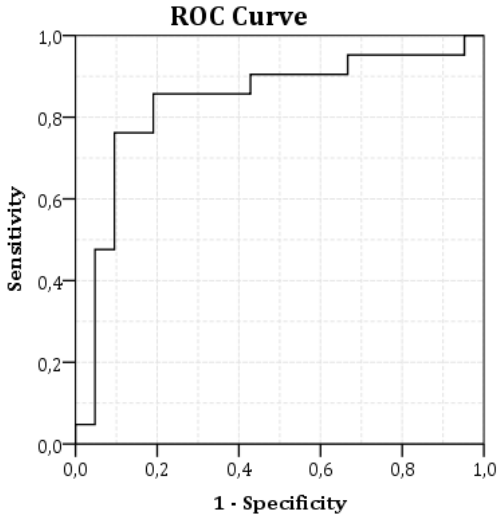

Figure 16: The ROC curve that was used to determine a cut-off value for the classification between healthy controls and pain controls, using the average theta/alpha ratio across the whole head. The cut-off value was determined by using Youden's index; this was the cut-off value whereby the sensitivity and the specificity of the classification were maximized. This resulted in a cut-off value of 0.94, whereby chronic pain patients were detected with a sensitivity of 76% and a specificity of 91%.

C.1 Specific brain areas: correlation matrices HC & PC

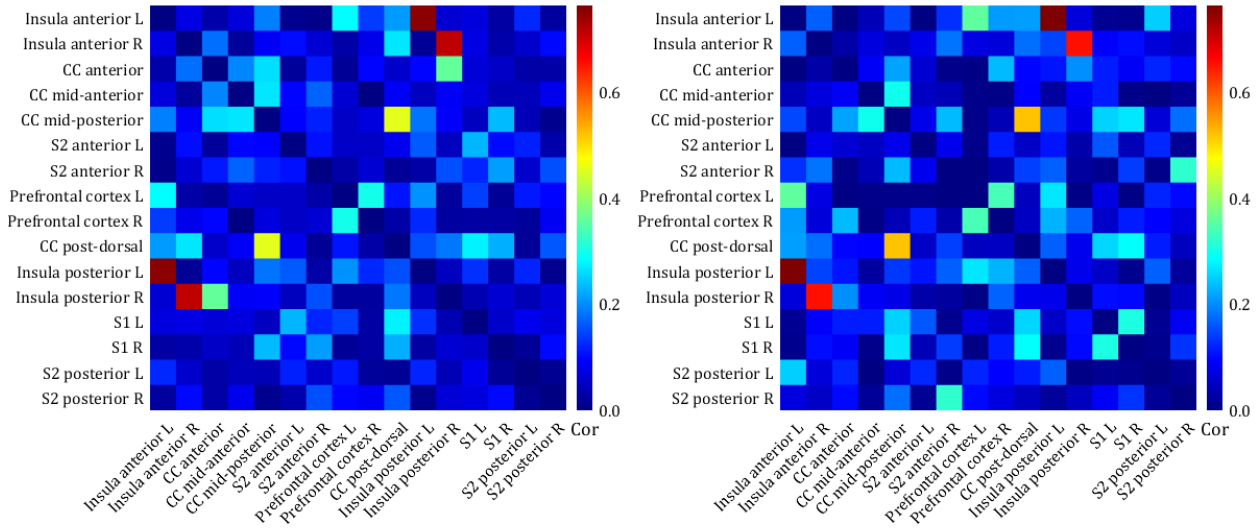

Figure 17: The correlation matrices for the healthy controls (left) and the pain controls (right), the values represent the absolute correlation. The correlation matrices of the two groups look very similar, the biggest difference is visible between the left and right primary somatosensory cortex. L = left, R = right, CC = cingulate cortex, S1 = primary somatosensory cortex, S2 = secondary somatosensory cortex.

C.2 Specific brain areas: coherence matrices high theta band and low alpha band

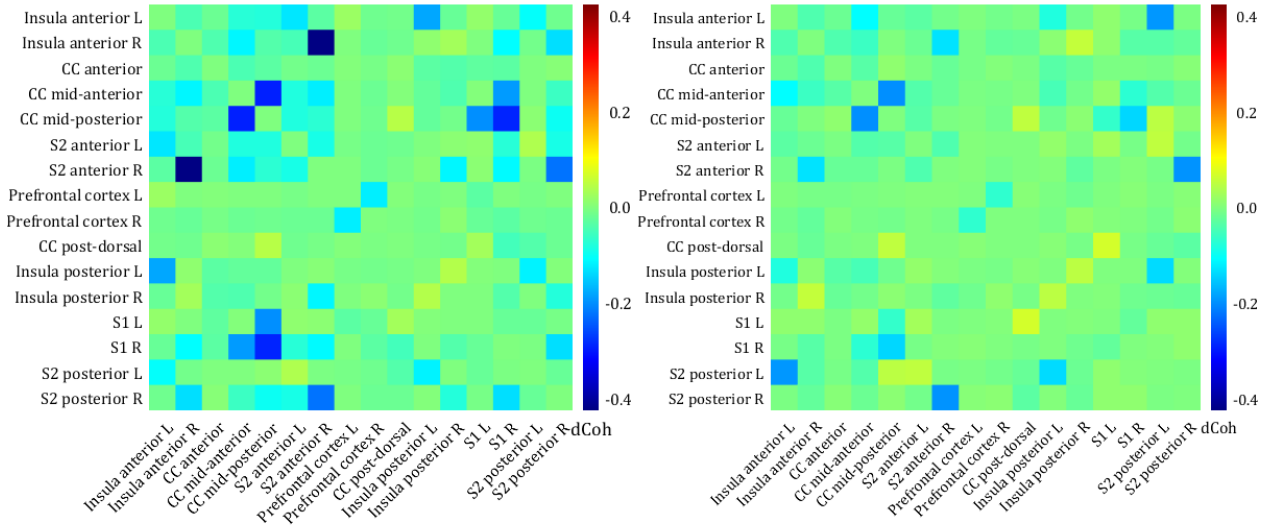

Figure 18: The coherence matrices for the high theta band (7-9 Hz, left) and the low alpha band (9-11 Hz, right), the values represent the average magnitude squared coherence for the high theta band and the low alpha band respectively. The coherence matrix for the low alpha band showed similar connectivity between the regions of interest as the coherence matrix for the high theta band, but coherence values were lower in the low alpha band. L = left, R = right, CC = cingulate cortex, S1 = primary somatosensory cortex, S2 = secondary somatosensory cortex.

C.3 Specific brain areas: coherence matrices high theta band HC & PC

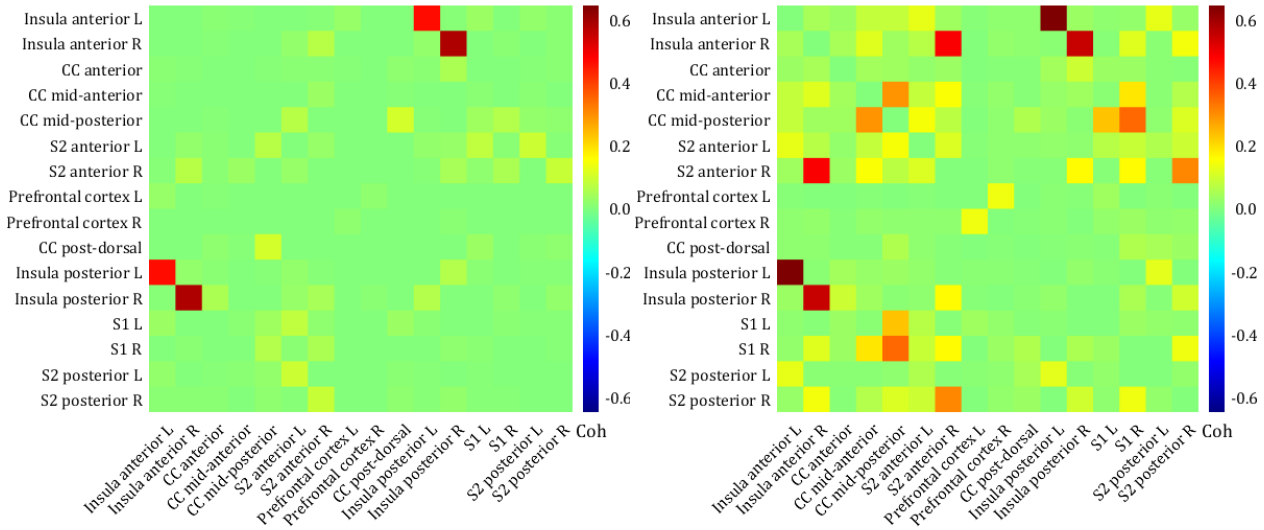

Figure 19: The coherence matrices for the healthy controls (HC, left) and the pain controls (PC, right), the values represent the average magnitude squared coherence for the high theta band (7-9 Hz). The coherence matrix for the HC showed generally low coherence values, except for the anterior insula. The coherence matrix for the PC showed higher coherence values between the regions of interest, especially between the right anterior insula and the right anterior S2. L = left, R = right, CC = cingulate cortex, S1 = primary somatosensory cortex, S2 = secondary somatosensory cortex.

C.4 Specific brain areas: correlation matrix with maximum across 5 minutes

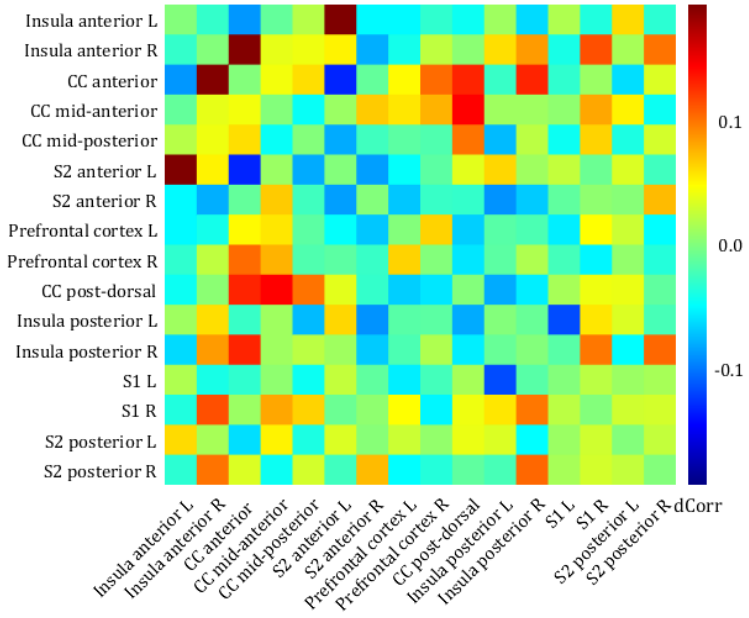

Figure 20: The difference in correlation between the HC and the PC, computed with the maximum correlation values across the five-minute recording. L = left, R = right, CC = cingulate cortex, S1 = primary somatosensory cortex, S2 = secondary somatosensory cortex.

D Alpha power distribution (sensor level): Spinal cord stimulation

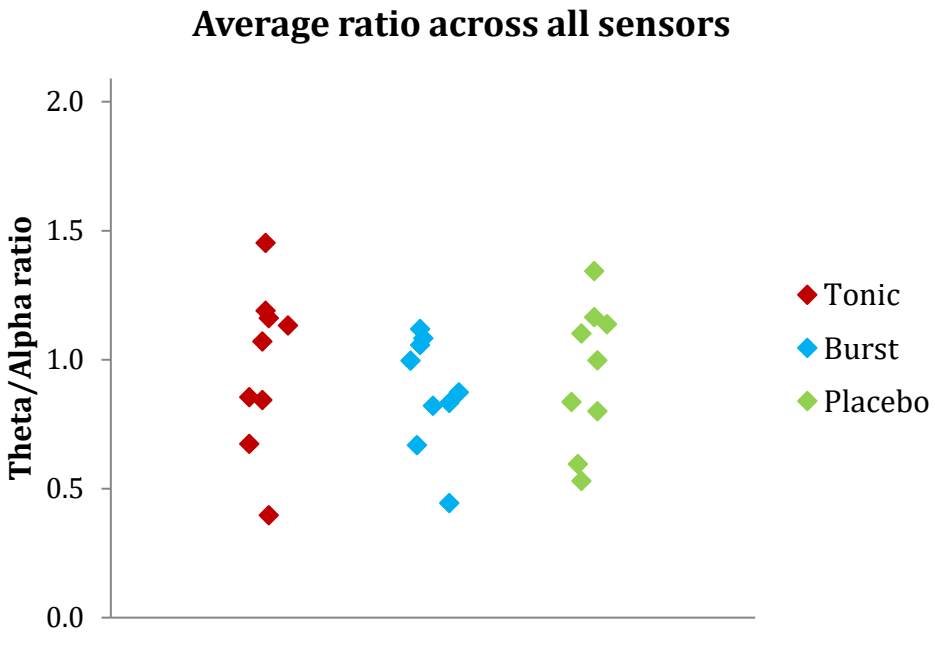

Figure 21: The average theta/alpha ratio across the whole head for the 9 patients with a spinal cord stimulator, after one-week evaluation periods of tonic, burst and placebo stimulation. The ratios were similarly distributed for each of the three stimulation settings.

E.1 Alpha power distribution (source level): tonic vs placebo stimulation

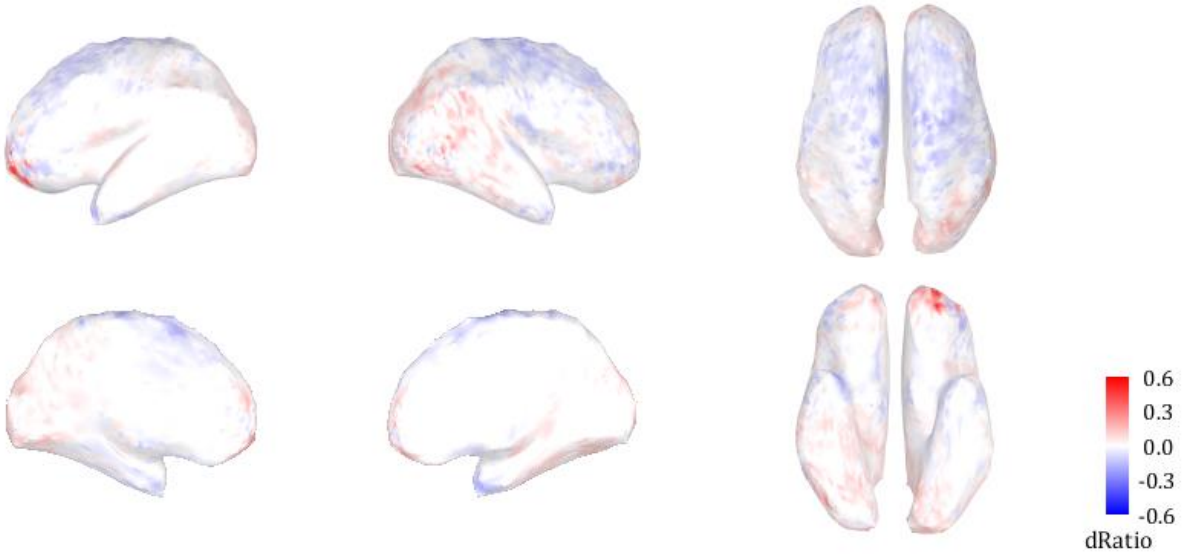

Figure 22: The difference in theta/alpha ratio (source level) between tonic stimulation and placebo stimulation. A positive difference means a higher ratio during tonic stimulation and a negative difference means a higher ratio during placebo stimulation.

E.2 Alpha power distribution (source level): burst vs placebo stimulation

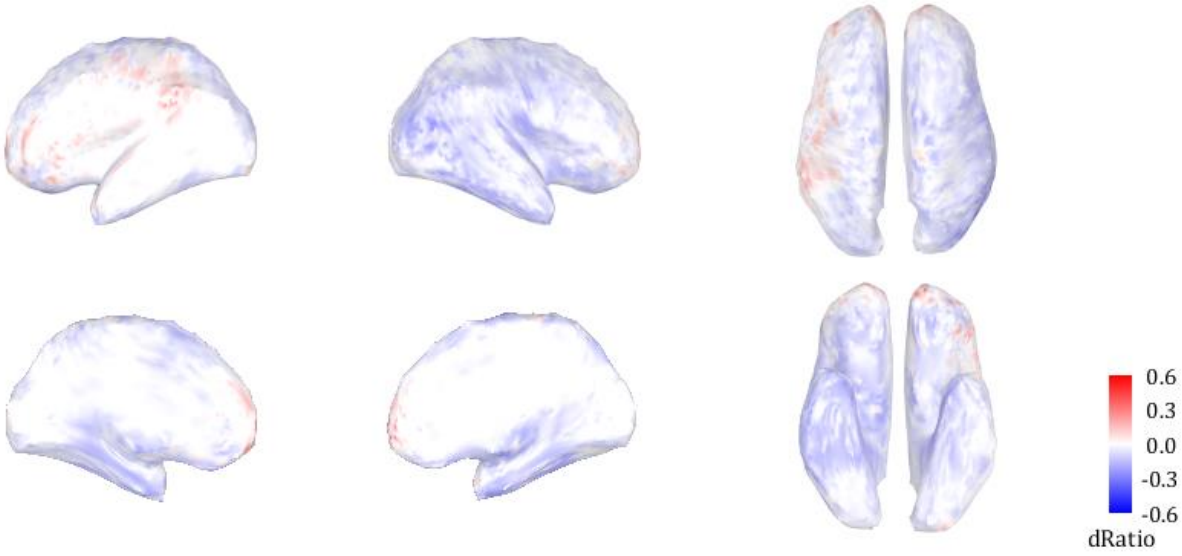

Figure 23: The difference in theta/alpha ratio (source level) between burst stimulation and placebo stimulation. A positive difference means a higher ratio during burst stimulation and a negative difference means a higher ratio during placebo stimulation.

E.3 Alpha power distribution (source level): Source model with thalamus

The source model revealed a significant difference in theta/alpha ratio between the healthy controls (HC) and the pain controls (PC, section 4.1.2). The most significant areas showed to be the cingulate cortex, and cortical areas caudal to the cingulate cortex. As this model could only project activity on the cortical areas, we hypothesized that the difference in activity could also originate from a source deeper than the cortex: the thalamus. However, source modelling of surfaces deeper than the cortex is more complex and warrants a different strategy. Also, the validity of modelling deeper sources is yet uncertain.

The vertices representing the thalamus were added to the cortical surface model that was already imported in Brainstorm. As the vertices of the thalamus represented current dipoles of deeper sources, the orientation of the current dipoles was set to unconstrained. This meant that the orientation was not set perpendicular to the cortical surface, but three orthogonal dipoles were used for each of the thalamic vertices (x, y and z). Subsequently a forward model was computed (overlapping spheres) and the minimum norm imaging method of Brainstorm was used to estimate the activity for each source. The theta/alpha ratio was then computed for each source and the differences between the HC and the PC were analyzed by using a permutation t-test with a false discovery rate (FDR) correction for the number of sources (p-values < 0.01 were assumed to be significant). The results for the thalamus were visualized in the form of a volume grid.

The thalamus indeed showed significantly higher theta/alpha ratios for the PC group, compared to the HC group (fig 20). The cortical sources, surrounding the thalamus, were not significantly different between the two groups anymore (compared to fig 6, section 4.1.2).

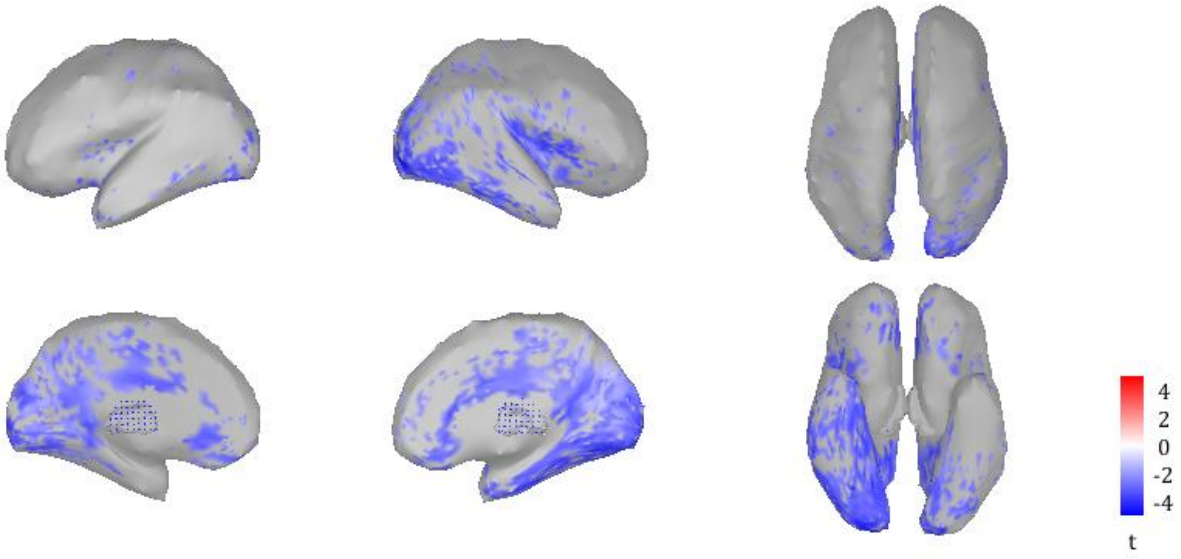

Figure 24: The results for a permutation t-test between the average (source level, with thalamus) theta/alpha ratios for the healthy controls and the average (source level) theta/alpha ratios for the pain controls. The results were false discovery rate (FDR) corrected for the number of sources. The values represented in the figure are t-values based on a significance level of p < 0.01. The areas which showed the largest differences between the two groups, were the insula (primarily the right insula), the cingulate cortex and the right temporal/occipital cortex.

F.1 Specific frequency bands: alpha1, tonic & burst stimulation

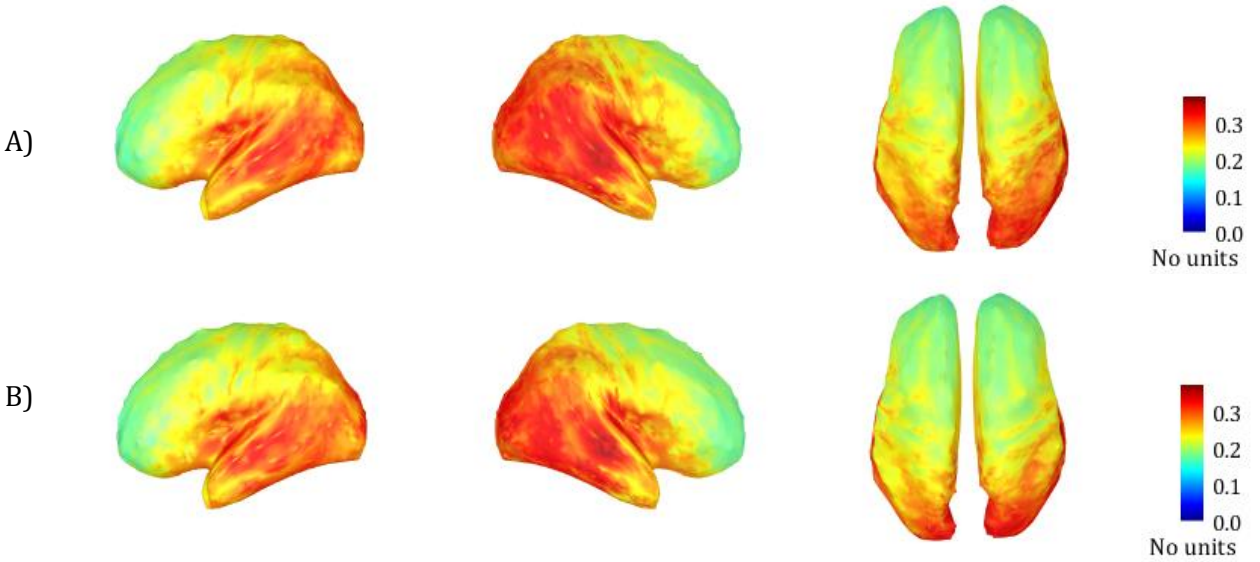

Figure 25: The mean relative power in the alpha1 frequency band (8-10 Hz) for every source, (A) for tonic stimulation and (B) burst stimulation. There are only small differences in cortical activity between the two different stimulation settings.

F.2 Specific frequency bands: alpha1, tonic & burst vs placebo stimulation

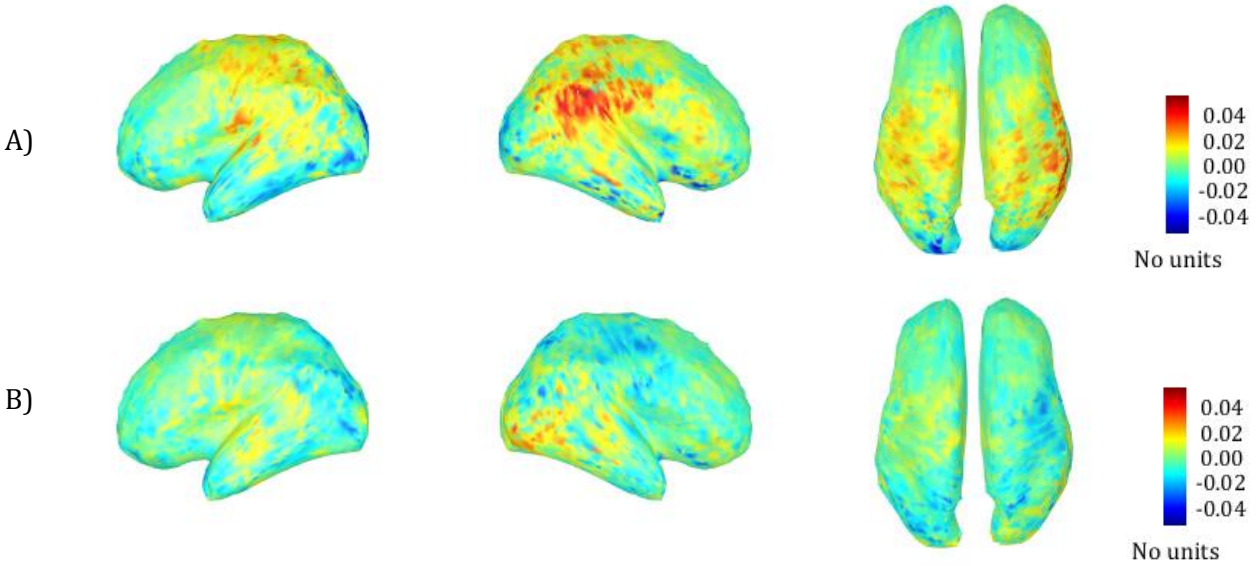

Figure 26: The difference in mean relative power in the alpha1 frequency band (8-10 Hz) for every source, (A) between tonic stimulation and placebo stimulation and (B) between burst stimulation and placebo stimulation. The positive values indicate more power in the alpha1 band for either tonic stimulation (A) or burst stimulation (B), compared to placebo stimulation. Especially the right hemisphere shows more alpha1 power in the somatosensory cortex and the parietal lobe for tonic versus placebo stimulation, this is not the case for burst versus placebo stimulation.

F.3 Specific frequency bands: beta1, tonic & burst vs placebo stimulation

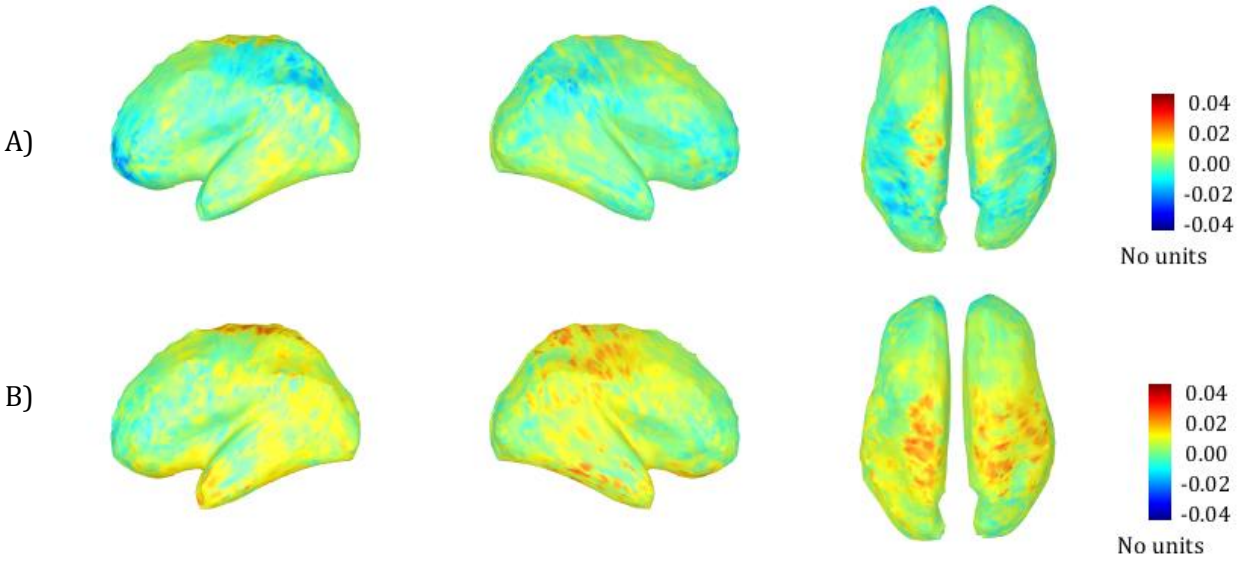

Figure 27: The difference in mean relative power in the beta1 frequency band (13-18 Hz) for every source, (A) between tonic stimulation and placebo stimulation and (B) between burst stimulation and placebo stimulation. The positive values indicate more power in the beta1 band for either tonic stimulation (A) or burst stimulation (B), compared to placebo stimulation. When comparing burst to placebo (B), there is more beta1 power in the somatosensory cortex during burst stimulation. When comparing tonic to placebo (A), there is no clear difference for that area.

F.4 Specific frequency bands: theta, tonic vs burst stimulation

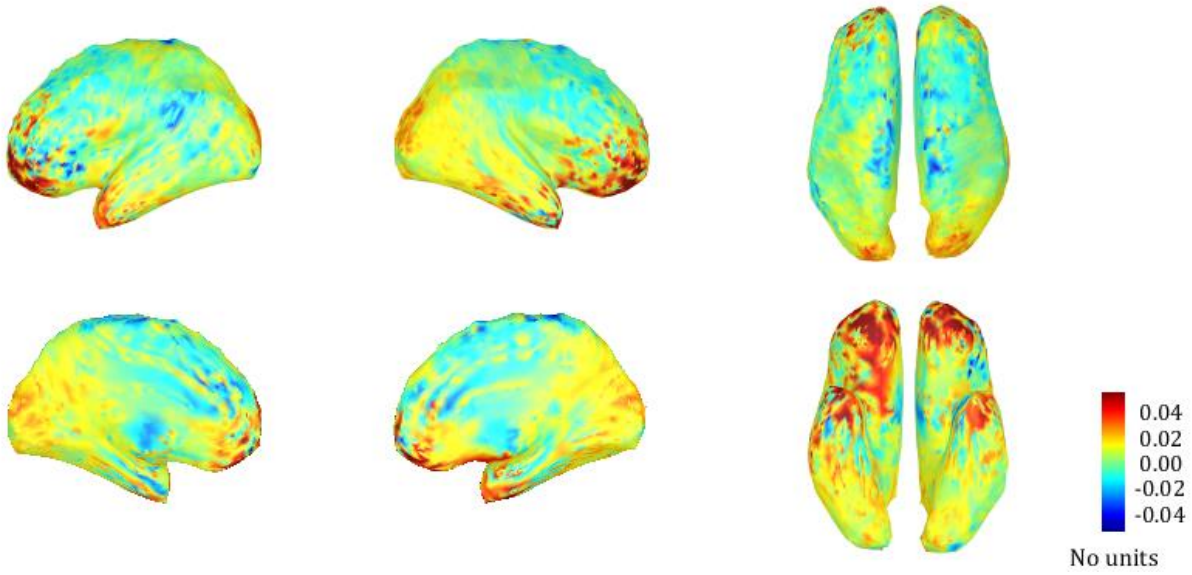

Figure 28: The difference in mean relative power in the theta frequency band (4-7.5 Hz) between tonic stimulation and burst stimulation for every source. The positive values indicate more power in the theta band during tonic stimulation, compared to burst stimulation. The prefrontal cortex of both hemispheres shows an increased theta power during tonic stimulation, compared to burst stimulation.